University of Alberta
Printing Department

THE UNIVERSITY OF ALBERTA

RECOMBINATION EFFECTS ON ELECTRON TUNNELING INTO SUPERCONDUCTING LEAD

BY

SHYAM MOHAN KHANNA

A THESIS

SUBMITTED TO THE FACULTY OF GRADUATE STUDIES IN PARTIAL FULFILMENT OF THE REQUIREMENTS FOR THE DEGREE OF MASTER OF SCIENCE

DEPARTMENT OF PHYSICS

EDMONTON, ALBERTA

NOVEMBER, 1965

UNIVERSITY OF ALBERTA

FACULTY OF GRADUATE STUDIES

The undersigned certify that they have read, and recommend to the Faculty of Graduate Studies for acceptance, a thesis entitled "RECOMBINATION EFFECTS ON ELECTRON TUNNELING INTO SUPERCONDUCTING LEAD", submitted by Shyam Mohan Khanna in partial fulfilment of the requirements for the degree of Master of Science.

ABSTRACT

Since the pioneering work of Giaever (1960 a,b), the electron tunneling technique has been successfully applied to the study of energy gap, quasi-particle density of states and phonon effects in superconductors.

Scalapino et al (1965) predicted a peak in the effective tunneling density of states in lead at non-zero temperatures due to recombination effects. Using the electron tunneling technique, we have obtained results for the variation with voltage of the normalized dynamic conductance of aluminum/aluminum oxide/lead tunnel junctions which agree well with their published work and give definite evidence for the occurrence of the recombination phenomena. The energy gap for lead was found to be $2\Delta(0)_{Pb} = (2.68 \pm 0.06)$ mev which is also in agreement with published results.

During the course of the present work, an interpolation formula for calibration of a germanium thermometer using only three known temperatures was obtained in the range of temperatures between 7.2° K and 0.52° K. The interpolated temperatures are accurate to $\pm 0.05^{\circ}$ K above 2.5° K and to nearly 1% below 2.5° K.

ACKNOWLEDGEMENTS

I wish to express my gratitude to Dr. S. B. Woods, my research supervisor, both for suggesting this project and for his cheerful encouragement and guidance throughout the course of this work.

I am indebted to Dr. J. P. Franck for many valuable discussions pertaining to both the research and the cryostat.

I also wish to thank Messrs. R. S. Seth and W. J. Keeler for their assistance during some of the runs.

Acknowledgements are also due to the technical staff of the Physics Department for advising or assisting in a number of problems that were encountered and for supplying the necessary liquid air and liquid helium.

Finally, it is a pleasure to acknowledge the alternating financial support of the Physics Department and the National Research Council during the course of this work.

TABLE OF CONTENTS

LIST OF FIGURES

CHAPTER I

INTRODUCTION

A. Motivation

This thesis reports an extension of work on the electron tunneling in superconductors which was initiated in this laboratory by Adler (1963).

According to the Bardeen-Cooper-Schrieffer theory of superconductivity (henceforth called the BCS theory) a forbidden energy gap appears about the Fermi energy in the density of electron states when a metal turns superconducting. The electron tunneling technique by which electrons of varying energies may be injected into a superconductor provides a direct and simple method of observing this energy gap. One can obtain not only the magnitude of the energy gap but also the variation of the density of states with energy outside the gap in a superconductor. Much smaller variations in the density of states above the energy gap have also been studied using the electron tunneling technique and have been identified as due to the predominant phonon energies of the metal. Thus, while providing a testing ground for the BCS theory and its modifications, this simple technique has also led to investigations of the phonon spectrum of several superconductors and holds promise of providing a great deal of information on

the properties of superconductors in general e.g. the double particle tunneling etc. (cf. chapter III).

The specimens used in the present work consisted of a thin insulating layer sandwiched between two thin metallic films. These specimens are ideally suited to low temperature work because of their small size. The current through the insulating layer was measured as a function of the voltage across it. If the potential difference across the layer is small, the current that tunnels through it is directly proportional to the potential difference as long as the density of states in the two metals is constant over the applied voltage range (cf. Fisher and Giaever 1961). When one or both of the metallic films turn superconducting, the density of states will vary rapidly in a small voltage range and the tunneling current will no longer vary linearly with the applied voltage. This non-linearity is related to variation in the density of states in the superconductor. In a metal/insulator/superconductor system (henceforth referred to as a N-S system) the normalised dynamic conductance σ, which is the ratio of the dynamic conductance $(\frac{di}{dv})_{ns}$ when one of the metallic members of the tunnel junction is superconducting to the dynamic conductance $(\frac{di}{dv})_{nn}$ when both members are normal, is measured as a function of applied

voltage v. A graph showing σ as a function of v directly displays the variation in the normalised density of states with energy in the superconductor. The normalised density of states in a superconductor is the ratio of density of states when a metal is superconducting, to the density of states when it is normal.

The purpose of the present work was to look for a peak in the effective tunneling density of states in lead predicted by Scalapino et al (1965) to be present at non-zero temperatures because of recombination processes that had been neglected in previous theoretical work.

CHAPTER II

MICROSCOPIC THEORIES OF SUPERCONDUCTIVITY

A. The BCS Theory

Superconductivity, first observed by Kamerlingh Onnes in 1911, is one of the most fascinating properties of metals. It was only in 1957 that the first successful microscopic theory, which explains most of general features of superconductivity, was proposed by Bardeen, Cooper and Schrieffer (1957 a,b).

The basic difficulty in constructing a theory of superconductivity is that the difference in energy between normal and superconducting phases -- the condensation energy -- is extremely small. Hence one has to pick out the terms in energy which differentiate between two phases and calculate this difference directly.

BCS theory has its origin in work of Cooper (1956) who was able to show that if there is a net attractive force between two electrons excited slightly above the Fermi surface, they can form a real bound pair ~~having a localized wave function~~. The energy of a system containing bound pairs is less than the ground state of the Fermi sea. Thus the ground state of the

Fermi sea is unstable against the formation of such Cooper pair states and the total energy would be reduced from that of the "normal" state. The BCS theory, then, provides a formalism for dealing with a state in which a large fraction of the electrons exist in such bound pairs.

The simplest way to describe the attractive force between a pair of electrons is based on virtual phonon exchange between them. The matrix element for scattering electrons from states $\vec{k}$ and $\vec{k}'$ to $\vec{k} + \vec{K}$ and $\vec{k}' - \vec{K}$ by exchange of a phonon is

$$\frac{2\hbar\,\omega_{\vec{q}}\;|\,M_{\vec{k},\,\vec{k}+\vec{K}}\,|}{(\epsilon_{\vec{k}} - \epsilon_{\vec{k}+\vec{K}})^2 - (\hbar\,\omega_{\vec{q}})^2} \qquad (2.1)$$

where $M_{\vec{k},\,\vec{k}+\vec{K}}$ is the matrix element of the electron-phonon interaction, $\hbar\,\omega_{\vec{q}}$ is the energy of the phonon involved and $\epsilon_{\vec{k}}$ is the Bloch state energy measured from the Fermi level. The interaction is attractive (negative) if

$$|\,\epsilon_{\vec{k}} - \epsilon_{\vec{k}+\vec{K}}\,| < \hbar\,\omega_{\vec{q}} \approx k_B\,\Theta_D \qquad (2.2)$$

where k_B is the Boltzmann constant and Θ_D is the Debye temperature. In this range of energies, the magnitude of expression (2.1) is roughly equal to

$$-\frac{2\,|\,M_{\vec{k},\,\vec{k}+\vec{K}}\,|^2}{\hbar\,\omega_{\vec{q}}} \qquad (2.3)$$

To this we have to add the repulsive Coulomb interaction ~~attraction~~ for which the matrix element would be

$$\frac{4\pi e^2}{K^2 + \lambda^2} \qquad (2.4)$$

where λ is a screening constant and e denotes the electronic charge.

The criterion for formation of bound pairs and superconductivity is that the attractive interaction dominates the screened Coulomb interaction. This criterion can be expressed in the form

$$-V = \left\langle -\frac{2\,|M_{\vec{k},\,\vec{k}+\vec{K}}|^2}{\hbar\,\omega_{\vec{q}}} + \frac{4\pi e^2}{K^2 + \lambda^2} \right\rangle \qquad (2.5)$$

$$< 0$$

where the average has been taken over electron states near the Fermi surface which satisfy Eqn. (2.2).

Since electrons follow Fermi-Dirac statistics, the matrix elements for all possible interactions which transfer two electrons from any two $\vec{k}$ values to any two others satisfying Eqn. (2.2) alternate in sign depending on the occupation number of other states which remain unchanged in the transition:

$$< \vec{k}_\alpha, \vec{k}_\beta \ . \ . \ . \ \vec{k}+\vec{K},\ \vec{k}'-\vec{K} \mid V \mid \vec{k}_\alpha,\ \vec{k}_\beta,\ . \ . \ . \ \vec{k},\ \vec{k}' >$$

$$= \pm < \vec{k}+\vec{K},\ \vec{k}'-\vec{K} \mid V \mid \vec{k},\ \vec{k}' > \quad .$$

The step taken by BCS is to associate all the $\vec{k}$ values in pairs $(\vec{k},\vec{k}')$ and require that either both or neither member of a pair be occupied. This will result in a single sign of the matrix element.

The momentum must be conserved in scattering processes. The maximum number of possible transitions, hence the lowest energy, can be obtained only when the momentum of each pair is the same so that any pair can be scattered into any other pair. Thus $(\vec{k} + \vec{k}') = \vec{C}$ should be same for all the pairs. For the ground state, the phase space available for transitions becomes maximum when the total momentum $\vec{C} = 0$. Further, as the exchange terms tend to reduce the (negative) interaction energy for pairs of parallel spin, it is most probable that the paired state should contain opposite spins. Thus the superconducting ground state can be expressed entirely in terms of paired states $(\vec{k}\uparrow\ ,\ -\vec{k}\downarrow)$ which are occupied simultaneously. The condensation energy of superconductivity will arise from interaction terms which scatter a given pair of electrons from one such paired state to another similarly paired state. Thus basically a two body correlation,

with strong preference for zero momentum singlet pairs, is the cause of superconductivity.

The Hamiltonian corresponding to this condensation energy - often referred to as the reduced Hamiltonian - of the system will be

$$H_{red} = T + V_{red} = 2\sum_{\vec{k}} \epsilon_{\vec{k}}\, b^{*}_{\vec{k}}\, b_{\vec{k}} - \sum_{\vec{k}\vec{k}'} V_{\vec{k}\vec{k}'}\, b^{*}_{\vec{k}'} b_{\vec{k}} \quad . \qquad (2.6)$$

Here T is the kinetic energy term, V_{red} is the interaction potential acting to scatter a Cooper pair from states $(\vec{k}\uparrow, -\vec{k}\downarrow)$ to $(\vec{k}'\uparrow, -\vec{k}'\downarrow)$ by an interaction strength $V_{\vec{k}\vec{k}'}$, , $b^{*}_{\vec{k}}$ and $b_{\vec{k}}$ are pair creation and annihilation operators defined by

$$b^{*}_{\vec{k}} = c^{*}_{\vec{k}\uparrow}\, c^{*}_{-\vec{k}\downarrow}$$

and (2.7)

$$b_{\vec{k}} = c_{-\vec{k}\downarrow} c_{\vec{k}\uparrow} \quad .$$

$c^{*}_{\vec{k}/\sigma}$ and $c_{\vec{k}/\sigma}$ are the creation and annihilation operators respectively for electrons in Bloch states with crystal momentum $\vec{k}$ and spin index σ. They satisfy the Fermi anticommutation rules and

$$n_{\vec{k}/\sigma} = c^{*}_{\vec{k}/\sigma}\, c_{\vec{k}/\sigma} \qquad (2.8)$$

is the number operator whose expectation value gives the probability that state $\vec{k}/\sigma$ is occupied.

BCS assume that the probability of a specific configuration of pairs is given by the product of probabilities of each individual pair state being occupied. Thus the ground state function Ψ_0 is

$$\Psi_0 = \prod_{\vec{k}} (u_{\vec{k}} + v_{\vec{k}} b^*_{\vec{k}}) \Phi_0 \qquad (2.9)$$

where Φ_0 is vacuum, $v^2_{\vec{k}}$ is the probability that the k^{th} pair is occupied and $u^2_{\vec{k}}$ is the probability that it is not occupied. Clearly

$$u^2_{\vec{k}} + v^2_{\vec{k}} = 1 \quad . \qquad (2.10)$$

The energy corresponding to the reduced Hamiltonian H_{red} for the state (2.9) is

$$W_c = 2 \sum_{\vec{k}} \epsilon_{\vec{k}} v^2_{\vec{k}} - \sum_{\vec{k}\vec{k}'} V_{\vec{k}\vec{k}'} u_{\vec{k}} v_{\vec{k}} u_{\vec{k}'} v_{\vec{k}'} \quad . \qquad (2.11)$$

Treating $v_{\vec{k}}$ as a variational parameter, the value of $v_{\vec{k}}$ which gives minimum value of W_c is

$$v^2_{\vec{k}} = \frac{1}{2} \left(1 - \frac{\epsilon_{\vec{k}}}{E_{\vec{k}}}\right)$$

and (2.12)

$$u^2_{\vec{k}} = \frac{1}{2} \left(1 + \frac{\epsilon_{\vec{k}}}{E_{\vec{k}}}\right)$$

where

$$E_{\vec{k}} = \sqrt{\epsilon^2_{\vec{k}} + \Delta^2_{\vec{k}}} \qquad (2.13)$$

and

$$\Delta_{\vec{k}} = \sum_{\vec{k}'} V_{\vec{k}\vec{k}'} v_{\vec{k}'} u_{\vec{k}'} \quad . \qquad (2.14)$$

It follows that

$$\Delta_{\vec{k}} = \sum_{\vec{k}'} \frac{V_{\vec{k}\vec{k}'}\, \Delta_{\vec{k}'}}{2\, E_{\vec{k}'}} \quad . \tag{2.15}$$

BCS make the following assumptions:

(a). (2.1) is taken to be constant given by (2.3) in the range where $|\epsilon_{\vec{k}}|$ and $|\epsilon_{\vec{k}+\vec{K}}|$ are less than $\hbar\omega_{\vec{q}}$ and zero elsewhere.

(b). An average value of (2.4) is used and is taken to be constant in the same range of energies as in (a) and zero elsewhere.

(c). $\Delta_{\vec{k}} \approx$ constant $= \Delta$ for $|\epsilon_{\vec{k}}| \leq \hbar\omega_{\vec{q}}$ and zero otherwise.

(d). The density of states $N(\epsilon_{\vec{k}})$ is assumed to be constant $N(0)$ in the range $|\epsilon_{\vec{k}}| \leq \hbar\omega_{\vec{q}}$.

With these assumptions Eqn. (2.15) reduces to

$$\Delta = \frac{\hbar\omega_{\vec{q}}}{\sinh\,(1/\,N(0)V)} \tag{2.16}$$

and the energy difference between normal and superconducting states, i.e. the condensation energy, is

$$W_s - W_n = W_c = -\frac{2\,N(0)(\hbar\omega_{\vec{q}})^2}{\exp\,[2/N(0)V] - 1} \quad . \tag{2.17}$$

Following Eqns. (2.12) and (2.13), the pair occupation function in the BCS ground state shown in Fig. 2.1(a) is seen to be like a Fermi function with $k_B T \approx \Delta_{\vec{k}}$. There are few holes deep in the Fermi sea and few highly excited pairs.

In the weak coupling limit, i.e. when $N(0)V \ll 1$, the energy gap at $T = 0^{\circ}K$ is found to be

$$2\Delta(0) = 3.52\, k_B T_c$$

where T_c is the transition temperature. For $0 < T < T_c$ the gap can be numerically calculated. The temperature dependence of the gap is shown in Fig. 2.2. The excitations involved in this calculation are discussed below.

B. Elementary Excitations and Density of States

A theory of superconductivity exactly equivalent to the BCS theory was formulated by Bogoliubov (1958) who introduced a new set of quasi-particle operators:

$$\gamma^*_{\vec{k}} = u_{\vec{k}}\, c^*_{\vec{k}} - v_{\vec{k}}\, c_{-\vec{k}}$$

and (2.18)

$$\gamma^*_{-\vec{k}} = u_{\vec{k}}\, c^*_{-\vec{k}} + v_{\vec{k}} c_{\vec{k}} \quad .$$

This transformation preserves the Fermi anticommutation rules. The BCS ground state is vacuum for these particles. These operators can create and destroy excitations of

Figure 2.1

(a) Pair occupation function in the BCS ground state.

(b) Quasi-particle energy in the superconductor.

(c) Quasi-particle energy in the normal metal.

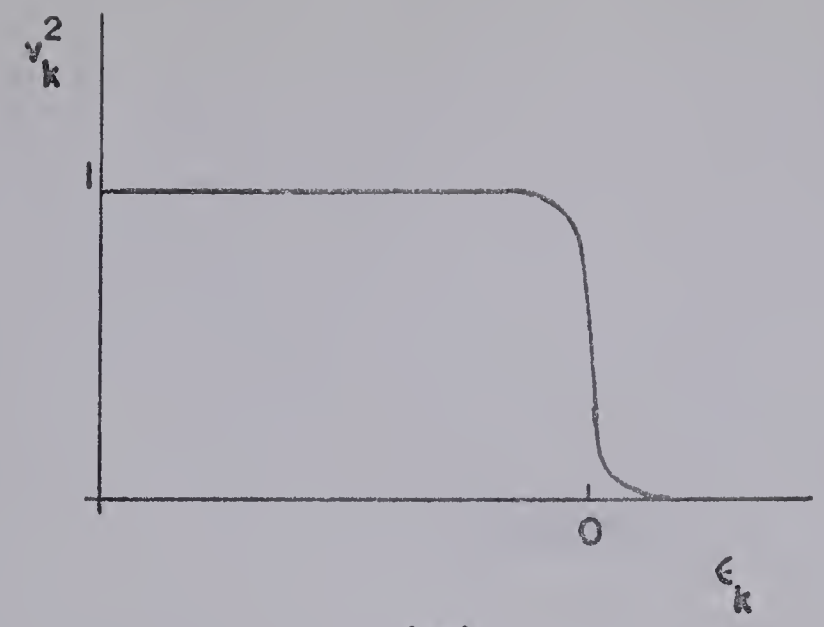

(a)

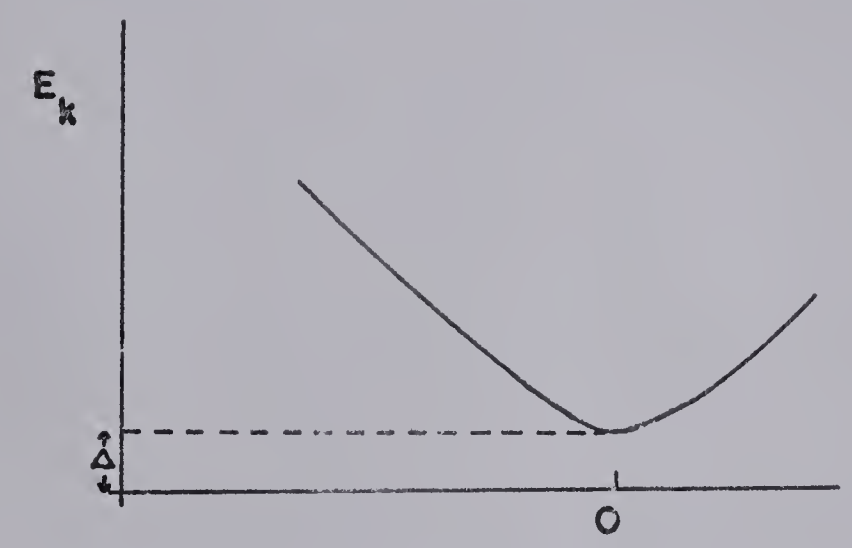

(b)

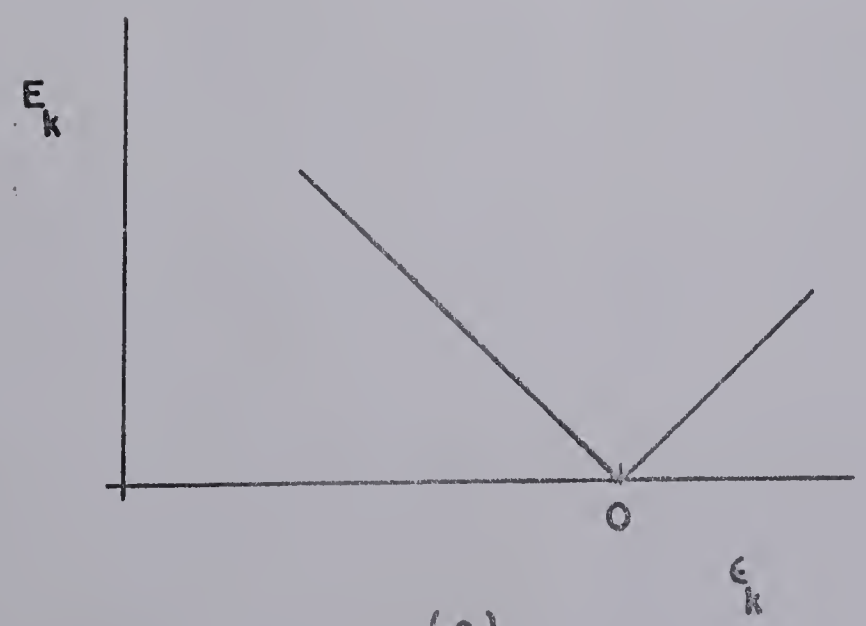

(c)

Figure 2.2

Temperature dependence of the energy gap.

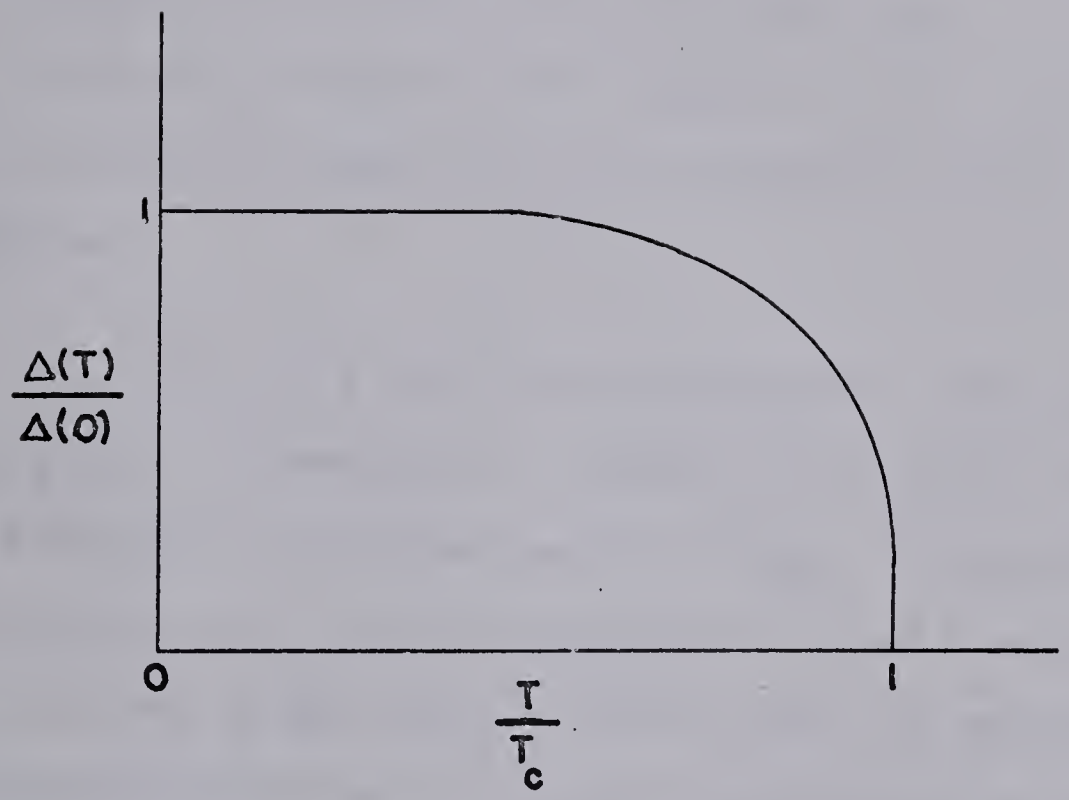
1
Δ(T)
Δ(0)
0
1
T
Tc

vacuum in the same manner as $c^*_{\vec{k}}$ and $c_{\vec{k}}$ can respectively "create" and "destroy" electrons. $\gamma^*_{\vec{k}}$ (or $\gamma_{-\vec{k}}$) always creates an excitation with net momentum $\vec{k}$ (or $-\vec{k}$) and spin up (or down). Using Eqns. (2.12) and (2.13), it is evident that these excitations of the superconducting state are peculiar quasi-particles which change from being like electrons ($\epsilon_{\vec{k}} \gg \Delta$) to being like holes ($\epsilon_{\vec{k}}$ negative and $|\epsilon_{\vec{k}}| \gg \Delta$) as they cross the Fermi surface at which they are an equal mixture of electrons and holes.

If Ψ_o is the BCS ground state, then $\gamma^*_{\vec{k}}\,\Psi_o$ and $\gamma^*_{-\vec{k}}\,\gamma^*_{\vec{k}}\,\Psi_o$ correspond to "single" and "pair" excitations with excitation energies $E_{\vec{k}}$ and $2\,E_{\vec{k}}$ corresponding to, respectively, one or both members of a pair being excited. Since excited single particles can only be produced in pairs, the minimum energy of an allowed excitation is $2\,\Delta$. The energy $E_{\vec{k}}$ of a quasi-particle in the superconducting and normal states is shown in Figs. 2.1(b) and (c). These excitations behave like independent fermions.

Assuming an isotropic energy gap, the density of excited states N(E) in a superconductor is,

$$N(E) = N(\epsilon)\,(dE/d\epsilon)^{-1}$$

where $N(\epsilon)$ is the density of states in the normal metal. As

$$E^2 = \epsilon^2 + \Delta^2 \qquad (2.13)$$

we have $N(E) = N(\epsilon) \cdot \dfrac{|E|}{\sqrt{E^2-\Delta^2} + \Delta\frac{d\Delta}{d\epsilon}}$

$$= N(0) \frac{|E|}{\sqrt{E^2 - \Delta^2}}$$

using the assumptions (c) and (d) stated earlier. As E cannot have values smaller than Δ,

$$\begin{aligned} N(E) &= 0 \qquad \text{if} \quad |E| < \Delta \\ &= N(0) \cdot \frac{|E|}{\sqrt{E^2 - \Delta^2}} \qquad \text{if} \quad |E| \geqslant \Delta . \end{aligned} \tag{2.19}$$

Thus N(E) is singular at the gap edges. At energies well above the gap, this expression reduces to N(0).

C. Modifications to BCS Theory

BCS theory, using only one adjustable parameter N(0)V, compares surprisingly well with experimental results. However, anisotropy in a given metal, differences between metals and structure in the superconducting density of states indicate need for improvement of this theory. In the isotropic model, this is achieved by replacing $V_{\vec{k}\vec{k}'}$ by a kernel $K(\epsilon,\epsilon')$ which has more accurate convergence properties at larger values of these variables. This leads to an energy gap function that depends on the energy in a complicated manner and which manifests itself in predictions of measurable quantities.

Deviations from BCS theory are more pronounced in cases where the weak coupling limit is not applicable.

In the BCS theory, the energy levels are assumed to have zero width so that it is not applicable when life time effects are to be considered. Eliashberg (1960) has included life time effects of these states and phonon distribution in extending the Bogoliubov theory with the use of Green's function methods. Following this treatment, the energy gap turns out to be a complex function of energy and has maxima and minima at energies close to Θ_D, $2\,\Theta_D$ etc., (henceforth we will take $\hbar = k_B = e = 1$ where these symbols have their usual meanings). Schrieffer et al (1963) have shown that Eliashberg formalism modifies the effective tunneling density of states in a superconductor which is now given by

$$N_T(E) = N(0)\ \mathrm{Re}\left\{\frac{|E|}{[E^2 - \Delta^2(E)]^{\frac{1}{2}}}\right\} \qquad (2.20)$$

where $\Delta(E)$ is a complex function of the energy.

CHAPTER III

THEORIES OF TUNNELING IN SUPERCONDUCTORS

In his pioneering work, Giaever (1960 a,b) studied the tunneling of electrons between a superconducting film and a normal one separated by an insulating layer which was a few tens of angstroms thick. Observations of current through a tunnel junction as a function of voltage with one or both of the films in the superconducting state provide one of the most direct measurements of the superconducting energy gap and give detailed information about the density of states and some other properties of superconductors.

A. Simple Model of Tunneling

It is well known that a current can pass between two metals separated by a thin insulating layer due to quantum mechanical tunneling of the electrons. (cf. Giaever and Fisher 1961). The treatment has been extended by Nicol et al (1960) and Giaever and Megerle (1961) for the case when one or both of the metals are superconducting. A good account of these theories has been given by Adler (1963).

In this model, the insulating layer in the tunnel junction is considered to be a potential barrier for the electrons. The transmission coefficient for an electron through this layer varies as exp $(-th^{\frac{1}{2}})$ where t is the insulating layer thickness and h ~~its~~ the height of potential barrier. These factors*(t and h) remain unaffected by the application of small voltages to the tunnel junction.

The probability of transition of an electron from an unoccupied state $\vec{k}_i$ on the left of the barrier to a state $\vec{k}_f$ on the right side (henceforth called metal 1 and metal 2 respectively) per unit time is

$$P_{\vec{k}_i \to \vec{k}_f} = 2\pi |M|^2 f_i (1 - f_f) N_f \qquad (3.1)$$

where M is the matrix element for the transition, f_i and f_f are the probabilities that initial and final states are occupied, and N_f is the density of final states.

The net tunneling current across the tunnel junction on application of voltage v is

$$i = 2\left[\int_{-\infty}^{\infty} 2\pi |M|^2 \left\{ N_1(E)\, f(E)\, \big(1-f(E+v)\big)\, N_2(E+v) - N_2(E+v)\, f(E+v)\, \big(1-f(E)\big)\, N_1(E) \right\} dE\right] \qquad (3.2)$$

---

* These parameters are reduced quantities so that the exponential factor is dimensionless.

where E is the energy measured from the Fermi level and f is the Fermi function. M is considered to be independent of the electron energy in the region of interest, that is, when $v \ll E_F$, E_F being the Fermi energy. The density of Bloch states near the Fermi level is assumed to be constant. In general, we can write

$$N_{ij}(E) = N_{in}(0)\, n_{ij}(E) \qquad (3.3)$$

where i refers to metal 1 or metal 2 and j to the normal (n) or superconducting (s) case and $N_{in}(0)$ represents the density of states at the Fermi level. We have

$$n_{in}(E) = 1$$

and

$$n_{is}(E) = R\ell \frac{|E|}{(E^2 - \Delta_i^2)^{\frac{1}{2}}} \quad . \qquad (3.4)$$

Using Eqns. (3.4) and (3.2), we obtain

$$\begin{aligned} i &= 4\pi |M|^2 \int_{-\infty}^{\infty} N_1(E)\, N_2(E+v)\, [f(E) - f(E+v)]\, dE \\ &= c \int_{-\infty}^{\infty} n_1(E)\, n_2(E+v)\, [f(E) - f(E+v)]\, dE \end{aligned} \qquad (3.5)$$

where $c = 4\pi |M|^2 N_{1n}(0)\, N_{2n}(0)$.

(i) Normal-Normal Case i_{nn}

In this case under the usual conditions of $v \ll E_F$ and $T \ll E_F$, the current reduces to

$$i_{nn} = cv. \tag{3.6}$$

$N_{1n}(0)$ and $N_{2n}(0)$ are considered to be constants. Fig. (3.1 a) illustrates the densities of states and occupation of levels in two normal metals near the Fermi surface at non-zero temperatures and shows the associated i-v characteristic.

(ii) Normal-Superconductor Case i_{ns}

When one of the two metals is superconducting, following BCS theory, the density of states then has an energy gap $2\Delta_1$ centered at the Fermi level. The corresponding density of states and i-v characteristic are shown in Fig. (3.1 b). In this case

$$\begin{aligned} i_{ns} &= c(v^2 - \Delta_1^2)^{\frac{1}{2}} \quad , \ |v| \geqslant \Delta_1 \\ &= 0 \qquad\qquad\qquad\quad , \ |v| < \Delta_1 \ . \end{aligned} \tag{3.7}$$

Also $i_{ns}(-v) = - i_{ns}(v)$.

Figure 3.1

Energy diagrams illustrating the density of states near the Fermi level, occupation of states and current-voltage characteristic in

(a) normal-normal case

(b) normal-superconductor case

(c) superconductor-superconductor case.

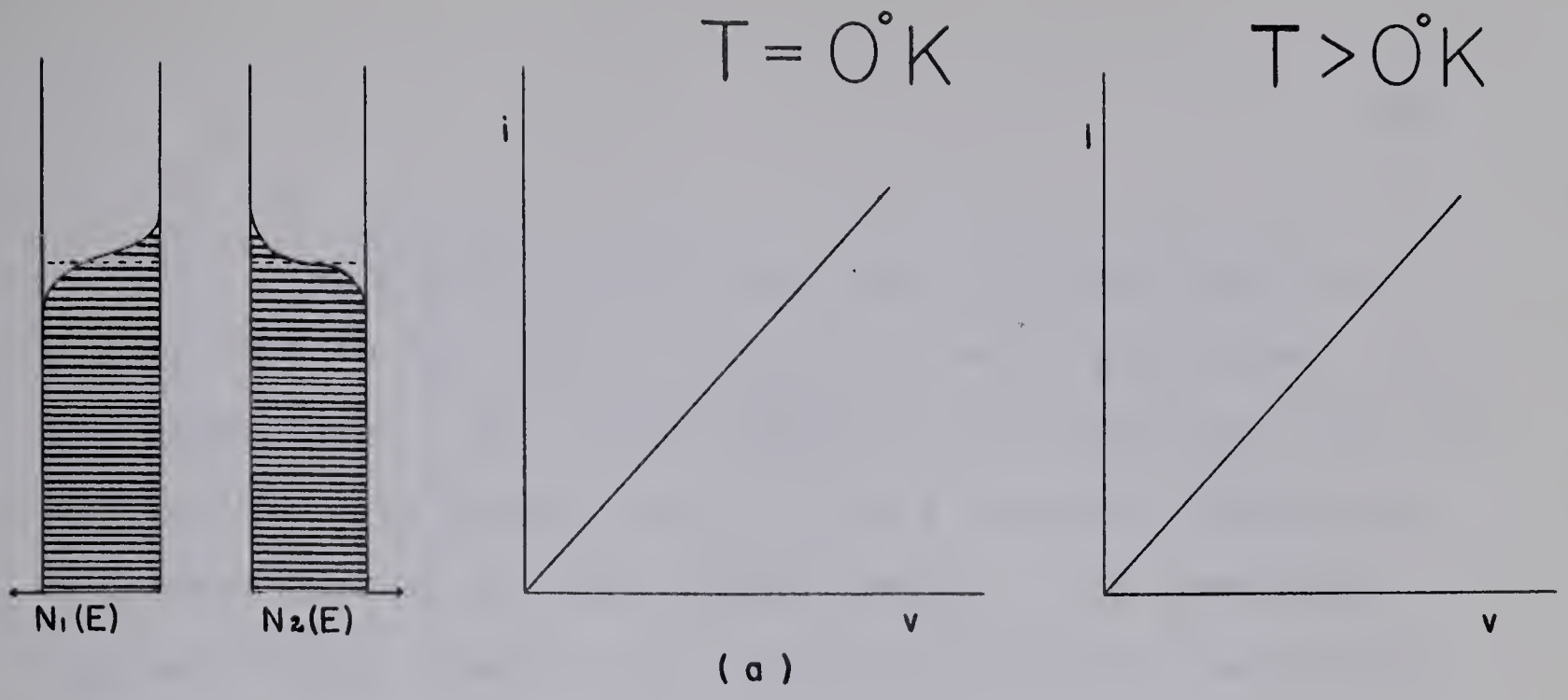
T = 0°K
T > 0°K
i
V
$N_1(E)$
$N_2(E)$
(a)
$2\Delta_1$
Δ_1
(b)
$2\Delta_2$
$2\Delta_1$
$\Delta_1+\Delta_2$
$\Delta_2-\Delta_1$
(c)
Unoccupied States
Occupied States

At $T \neq 0^{\circ}K$, there is a small current even for $v < \Delta_1$ due to the excited "electrons" which can tunnel into the other metal. As the two sides of the insulating layer now look entirely different, we will get a strongly temperature dependent current in this voltage region. The energy gap parameter will, however, be almost unambiguously measurable despite thermal smearing at $v \approx \Delta_1$ provided $T \ll \Delta_1$.

(iii) Superconductor-Superconductor Case i_{ss}

The corresponding "electron" density and i-v characteristic are shown in Fig. (3.1 c). There are energy gaps $2\Delta_1$ and $2\Delta_2$ centered at the Fermi levels of the two superconductors. Shapiro et al (1962) have studied this case at different temperatures.

At $T = 0^{\circ}K$, current i_{ss} will be zero as long as the applied voltage is less than $\Delta_1 + \Delta_2$. At $v = \Delta_1 + \Delta_2$, it will increase sharply and will approach i_{nn} at higher voltages. However, at a non-zero temperature, some current will flow at the smallest applied voltage due to excited "electrons" above the gaps. This current will increase until v attains the value $\Delta_2 - \Delta_1$ (with $\Delta_2 > \Delta_1$). With further increase in voltage, this current will decrease as the same number of "electrons" are available for tunneling as in range

$v < \Delta_2 - \Delta_1$, but into a lower density of available states in the opposite superconductor. This decrease in current continues until v is just less than $\Delta_1 + \Delta_2$. As illustrated in Fig. (3.1 c), at $v = \Delta_1 + \Delta_2$, the current rises sharply with voltage and finally approaches the value i_{nn}. Calculations of Shapiro et al (1962) show that the singularity at $v = \Delta_2 - \Delta_1$ is actually logarithmic and there is a discontinuous current jump at $v = \Delta_1 + \Delta_2$. However, allowance has to be made for the factors, e.g., life time and anisotropy effects, neglected in the BCS theory and experimentally we instead observe a cusp-like peak and a current jump spread over a small voltage interval. However due to piling up of states at the edges of the energy gaps in both superconductors, the "k_BT" smearing is of much less importance in this case than in a N-S system.

B. Modifications of the Simple Tunneling Model

Harrison (1961) has shown that band structure in normal metals cannot be observed through tunneling experiments. This is because the density of states is inversely proportional to the group velocity of electrons in an independent particle picture and thus the density of states in normal metals completely drops out in the tunneling current expression Eqn. (3.5). In a superconductor, however, this independent

quasi-particle model is not true. In this case, following Bardeen (1961), the matrix element still involves the group velocity of the normal electrons and not of the superconducting quasi-particles whereas the density of states involved in the transition is obviously that for the quasi-particles. Since the matrix element M is essentially unchanged, the only significant change in the tunneling current, due to the transition of at least one of the two metals of the tunnel junction to the superconducting state, comes from the density of states factor for the quasi-particles in a superconductor and it is this alone that we observe in the electron tunneling experiments.

After Bardeen's treatment, Cohen et al (1962) described the tunneling of electrons through a tunnel junction in terms of an effective Hamiltonian

$$H = H_1 + H_2 + H_T \tag{3.8}$$

where H_1 and H_2 are exact Hamiltonians for the metals 1 and 2 respectively and H_T is an operator which transfers electrons from one to the other.

$$H_T = \sum_{kk's} [M_{kk'} c^{*(2)}_{k's} c^{(1)}_{ks} + M_{k'k} c^{*(1)}_{ks} c^{(2)}_{k's}] \tag{3.9}$$

where $c^{(1)}_{ks}$ and $c^{*(2)}_{k's}$ destroy and create electrons in Bloch states of momentum $\vec{k}$ and $\vec{k}'$ respectively; s denotes the spin.

Schrieffer, Scalapino and Wilkins (1963) treated H_T as a small perturbation on the zero order Hamiltonian

$$H_o \equiv H_1 + H_2 \quad . \tag{3.10}$$

Starting with zero temperature, if $|O_1\rangle$ and $|O_2\rangle$ are the ground states of H_1 and H_2 respectively, $|O_1\rangle|O_2\rangle$ is the ground state of H_o as H_1 and H_2 are assumed to commute. Using first order perturbation theory, the transition probability per unit time for an electron from metal 1 to metal 2 is

$$\omega_{1\to 2} = 2\pi \sum_{\alpha,\beta} |\langle\alpha_1|\langle\beta_2| \sum_{kk's} M_{kk'} c^{*(2)}_{k's} c^{(1)}_{ks} |O_1\rangle|O_2\rangle|^2 \cdot \delta(\epsilon_\alpha+\epsilon_\beta-v) \tag{3.11}$$

where $|\alpha_1\rangle$ and $|\beta_2\rangle$ are the eigen-states of H_1 and H_2 in absence of perturbation and applied voltage v. ϵ_α is the energy difference between states $|\alpha_1\rangle$ and $|O_1\rangle$. ϵ_β has a similar meaning.

Assuming $M_{kk'}$ to be constant in the energy range of interest ($v \ll E_F$), we can write the transition rate and hence the current as

$$i \propto \int_o^v N^{(2)}_{T+}(E)\, N^{(1)}_{T-}(v-E)\,dE \tag{3.12}$$

where

$$N_{T+}^{(2)}(E) = \sum_{k',\beta} | <\beta_2 | c_{k's}^{*(2)} | 0_2> |^2 \delta(\epsilon_\beta - E)$$

and (3.13)

$$N_{T-}^{(1)}(E) = \sum_{k,\alpha} | <\alpha_1 | c_{ks}^{(1)} | 0_1> |^2 \delta(\epsilon_\alpha - E).$$

$N_{T\pm}^{(i)}(E)$, (i = 1,2) is the effective tunneling density of states for adding electrons (+) or holes (-).

Essentially, electron interaction through phonons is not instantaneous. Particle damping effects due to phonon emission also have to be taken into account. In a simple case, when these factors are ignored, one obtains from Eqn. (3.13) (see e.g. Schrieffer 1964)

$$N_{T\pm}(E) = N(0) \frac{|E|}{(E^2 - \Delta^2)^{\frac{1}{2}}} \quad . \qquad (2.19)$$

It is to be noted that $N_{T\pm}$ are just the same density of quasi-particle states used in the simple model earlier.

In real metals, Schrieffer et al (1963) using Green's function techniques have taken into account a non-instantaneous potential for electron interaction through phonons and have found a very simple expression for $N_{T\pm}(E)$

$$N_{T\pm}(E) = N(0)\ \mathrm{Re}\ \left[\frac{E}{(E^2 - \Delta^2(E))^{\frac{1}{2}}}\right] \quad . \qquad (2.20)$$

(cf. Eqn. (2.19)).

Δ is now a complex function of energy E, the imaginary part of which arises from damping effects caused by real phonon emission. For $E >> \Delta$, Eqn. (2.20) becomes

$$N_{T\pm}(E) \simeq N(0) \left[1 + \frac{\Delta_1^2(E) - \Delta_2^2(E)}{2E^2} + \ldots\right] \tag{3.14}$$

where

$$\Delta(E) = \Delta_1(E) + i\,\Delta_2(E) \quad , \; i = \sqrt{-1} \; .$$

This theory has been further extended to non-zero temperatures by Schrieffer (1964).

We are perhaps now in a position to draw a clearer picture of tunneling phenomenon in a superconductor which will also explain the complete absence of any coherence effects. It is important to note that in the tunneling process, there are two channels $\vec{k}$ and $\vec{k}'$ such that $\vec{k}'$ is above and $\vec{k}$ is below the Fermi level with $E_{\vec{k}} = E_{k'}$. In a N-S system as shown in Fig. (3.2), an electron in a state $\vec{k}\uparrow$ below the Fermi level in the normal metal can tunnel into a state $\vec{k}'\uparrow$ above the Fermi level in the superconductor with a probability $u_{k'}^2$, which is the probability that the pair state $(\vec{k}'\uparrow \; , \; -\vec{k}'\downarrow)$ is unoccupied (see Eqns. (2.12) and (2.13)). It can also tunnel into a state $\vec{k}\uparrow$ where states $\vec{k}'\uparrow$ and $\vec{k}\uparrow$ are related by $\epsilon_{k'} = -\epsilon_{\vec{k}}$. The probability of tunneling through this

Figure 3.2

Two possible final states for a given initially occupied state $\vec{k}\uparrow$ in a N-S system.

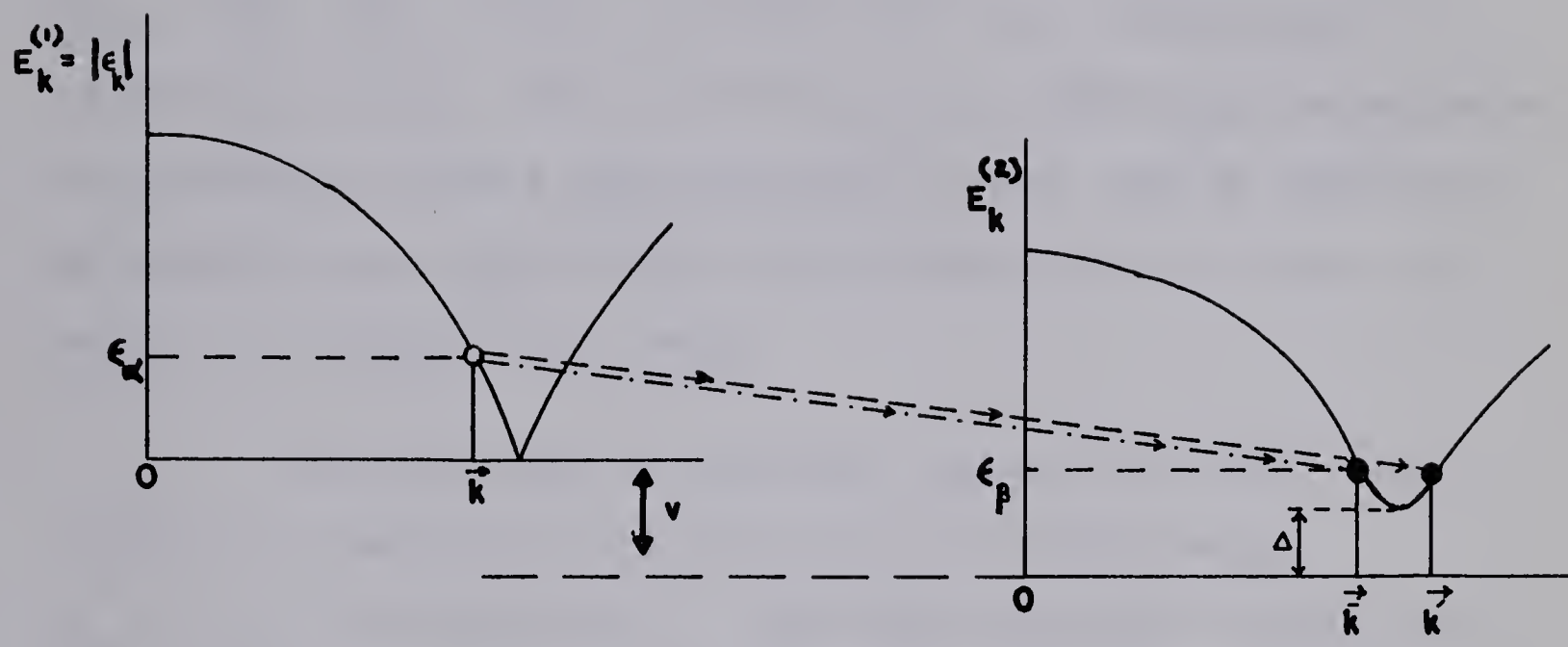

○ Unoccupied State

● Occupied State

channel is u_k^2 which is the probability that the pair state $(\vec{k}\uparrow , -\vec{k}\downarrow)$ is unoccupied. Since $\epsilon_{k'} = -\epsilon_{\overline{k}}$, u_k^2 equals $v_{k'}^2$. Thus the total probability that the electron can enter either state is $u_{k'}^2 + u_k^2 = u_{k'}^2 + v_{k'}^2 = 1$. This is also true when holes are to be injected and we then have $v_{k'}^2 + v_k^2 = v_{k'}^2 + u_{k'}^2 = 1$ for the total probability of injecting a hole. This is the physical origin of cancellation of coherence effects and tunneling current may be calculated by summing over all states in the superconductor above (or below) the Fermi level only.

Further when an electron leaves the normal metal, a hole is created in it giving an excitation energy $\epsilon_\alpha = |\epsilon_k|$ for this metal. When this electron occupies the state $\vec{k}'\uparrow$ in the superconductor, an excitation energy $\epsilon_\beta = E_{k'}$ is given to the superconductor. This can occur only if $v = |\epsilon_k| + E_{k'}$. Clearly the current will begin at $v = \Delta$.

In a S-S system, shown in Fig. (3.3), an electron from $\vec{k}\uparrow$ in superconductor 1 can tunnel into $\vec{k}'\uparrow$ or $\vec{k}''\uparrow$ and the total probability that it can enter either state is unity as before. An electron $\overline{\vec{k}}\uparrow$ with energy $\epsilon_k = -\epsilon_{\overline{k}}$ could also tunnel to the same final states. The total probability that an electron is available for tunneling in any of these initial states is that pair states $(\vec{k}\uparrow , -\vec{k}\downarrow)$ and $(\overline{\vec{k}}\uparrow , -\overline{\vec{k}}\downarrow)$

Figure 3.3

Two possible final states for each of the two initially occupied states $\vec{k}\uparrow$ and $\overrightarrow{-k}\uparrow$ in a S-S system.

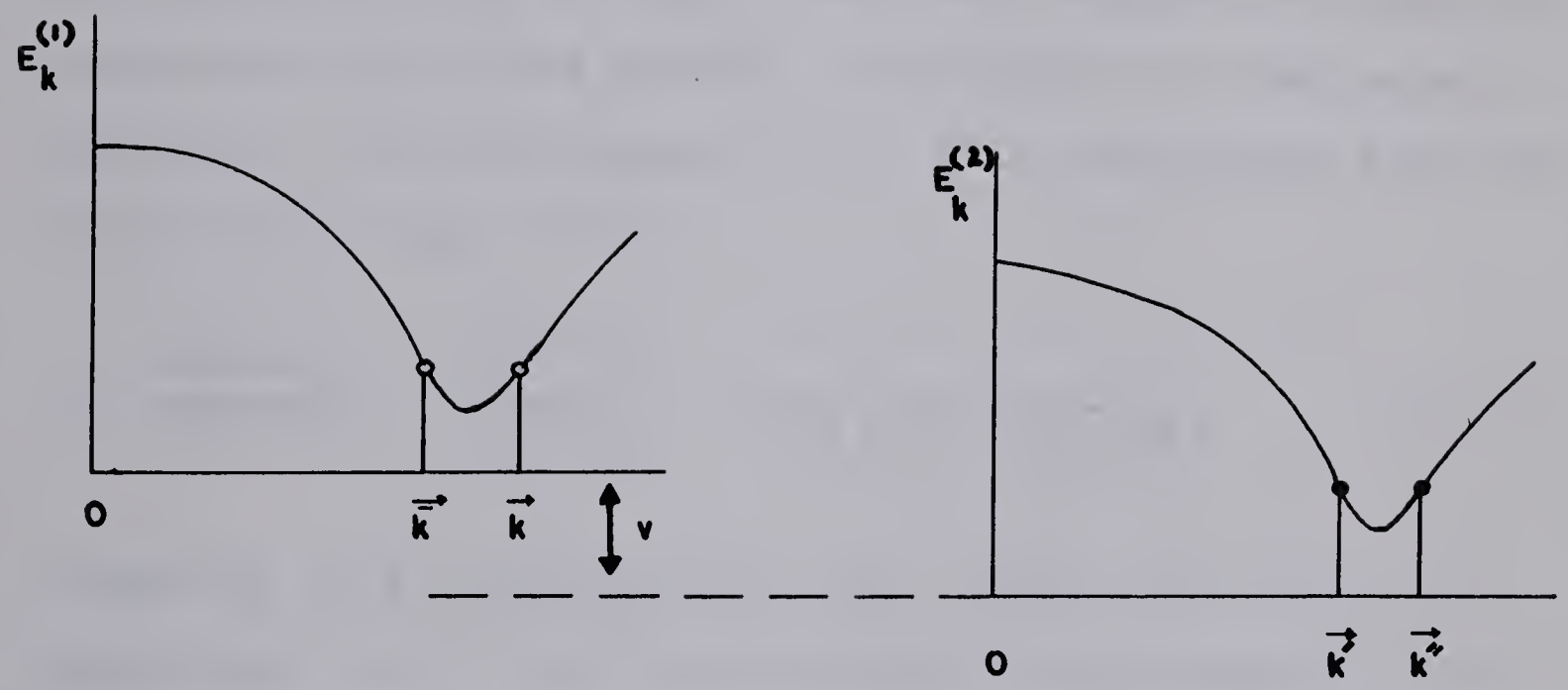

○ Unoccupied State

● Occupied State

are occupied, i.e. $v_k^2 + v_{\bar{k}}^2 = v_k^2 + u_k^2 = 1$. Thus in both initial and final states, coherence effects are not present. At $T = 0^{\circ}K$, as in a N-S system, tunneling current is possible only when $v \geqslant v_{min}$ where $v_{min} = \Delta_1 + \Delta_2$.

The dynamic conductance $(\frac{di}{dv})$ of a tunnel junction is obtained by taking the derivative of Eqn. (3.12). The ratio of $(\frac{di}{dv})_s$, when one of the metals in a tunnel junction is superconducting, to $(\frac{di}{dv})_n$ when both metals are normal is called the normalised dynamic conductance σ of the tunnel junction. For a N-S system at $T = 0^{\circ}K$, one obtains from Eqn. (3.12) using Eqn. (2.20)

$$\sigma = \frac{(di/dv)_s}{(di/dv)_n} = \frac{N_T^{(1)}(v)}{N_T^{(1)}(0)} = \mathrm{Re}\left[\frac{v}{\{v^2 - \Delta^2(v)\}^{\frac{1}{2}}}\right] . \qquad (3.15)$$

Comparing this expression with Eqn. (2.20), one notes that measurement of σ will provide detailed information of the superconducting tunneling density of states that in turn is a function of the gap parameter which is energy dependent.

C. Double Particle Tunneling in Superconductors

Taylor and Burstein (1963) observed currents between two superconductors at low temperature in excess of the usual current associated with single particle tunneling (referred to

as spt hereafter) discussed above. These excess currents were found to be independent of temperature and polarity and appeared with a sharp jump at $v = \Delta_1(T)$ and at $v = \Delta_2(T)$. An explanation has been proposed by Schrieffer and Wilkins (1963) in terms of a double particle tunneling (henceforth called dpt) mechanism involving a pair dissociation or recombination.

In a dpt process, two particles which form a condensed pair in either initial or final state are transferred across the insulating layer. In a typical process, shown in Fig. (3.4 a), which begins at $v = \Delta_1(T)$, two electrons are extracted from superconductor $S^{(1)}$. After tunneling to $S^{(2)}$, they recombine adding a condensed pair to $S^{(2)}$. Thus no excitations are created in $S^{(2)}$. In sum total, this leaves behind two quasi-particles in $S^{(1)}$ and the minimum energy required for the onset of this process is

$$2v = E^{(1)}_{k_1} + E^{(1)}_{k_2} = 2\Delta_1(T) \quad . \qquad (3.16)$$

Similarly a second process, shown in Fig. (3.4 b), involves removal of a condensed pair from $S^{(1)}$ which tunnels to form two quasi-particle states $\vec{k}_1$ and $\vec{k}_2$ in $S^{(2)}$. Thus no excitations are created in $S^{(1)}$. The threshold energy for this mechanism is

Figure 3.4

Two mechanisms contributing to double particle tunneling processes between two superconductors.

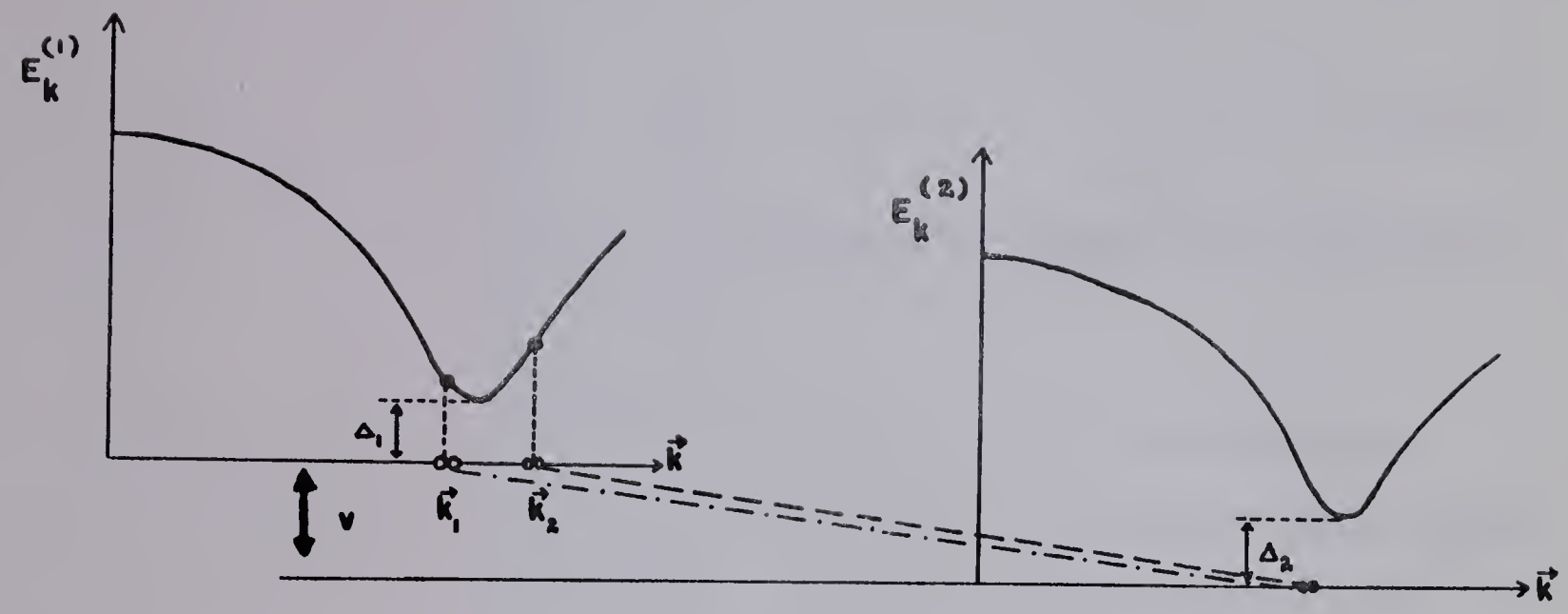

(a)

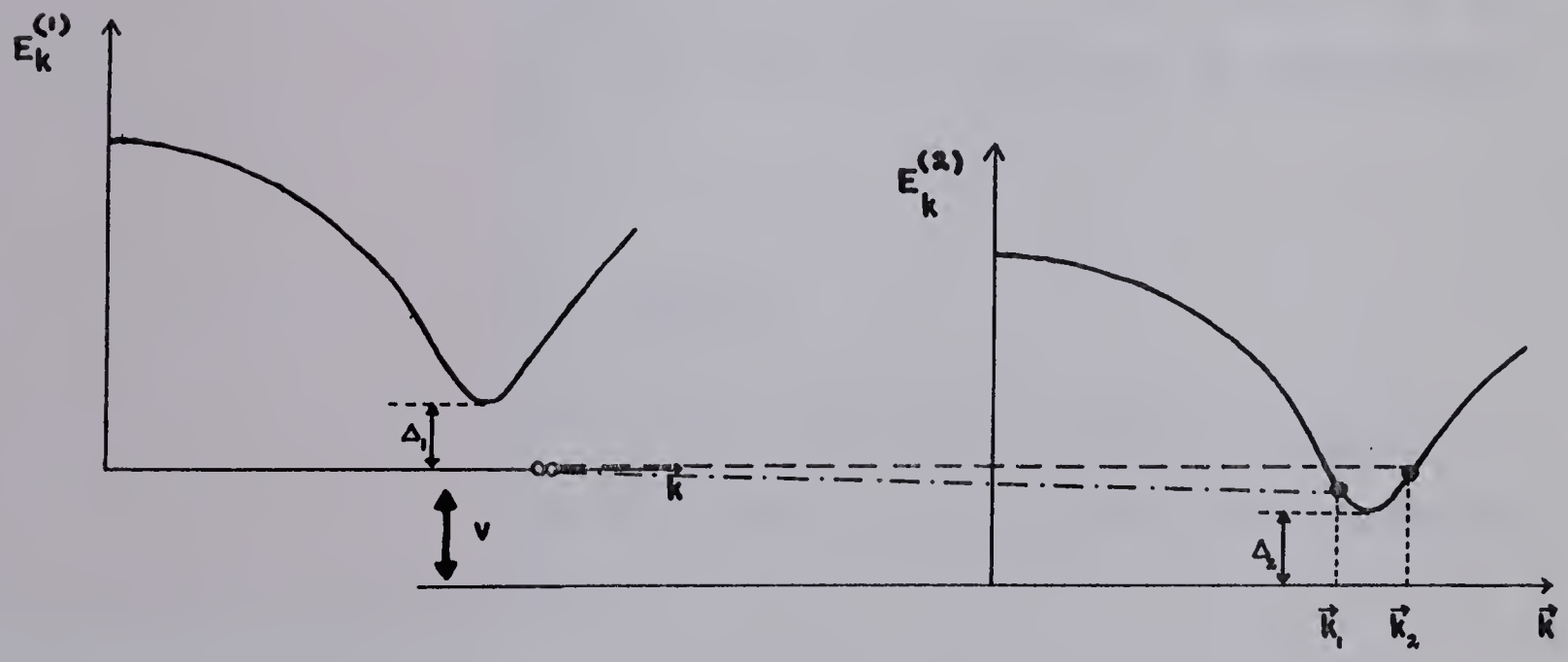

(b)

o Unoccupied State

• Occupied State

oo Pair State

$$2v = E_{k_1}^{(2)} + E_{k_2}^{(2)} = 2\Delta_2(T) \quad . \tag{3.17}$$

This explanation leads to temperature insensitive, polarity independent excess currents as observed.

These processes involve a second order matrix element and should result in far smaller currents than those observed for spt processes. However, as Schrieffer and Wilkins (1963) point out, the effective thickness of the insulating layer for the dpt and spt processes could be different leading to significant dpt currents. Such an abnormality in the apparent thickness of the insulating layers involved in dpt processes has been supported by experiments due to Adkins (1963).

D. Phonon Density of States

It was pointed out in Chapter I that the phonon density of states is reflected as structure in the dependence of σ on v. At energy

$$v = \Delta_o + \omega^{\lambda} \tag{3.18}$$

where Δ_o is the gap parameter at the edge of the energy gap and ω^{λ} is the transverse or longitudinal phonon peak energy, excited electron states may readily decay by phonon emission

to the increased density of available states at the gap edge. As pointed by Schrieffer et al (1963), this strong phonon emission rate produces a sharp decrease in the σ:v curve due to a rapid increase of Δ_2 and slight decrease in Δ_1 (see Eqn. (3.14)). Thus a sharp drop of σ indicates a peak in the density of states of phonons.

E. Recombination Processes in Lead

Scalapino, Wada and Swihart (1965) and Swihart, Scalapino and Wada (1965) have recently calculated the energy dependence of the gap parameter at non-zero temperatures for Pb which is a strongly coupled superconductor. They have used the same phonon distribution and Coulomb pseudopotential as used by Schrieffer et al (1963) which is in good agreement with tunneling experiments of Rowell et al (1963). However, in Pb, Scalapino et al (1965) estimated the electron phonon coupling constant α_ℓ^2 for longitudinal phonons to be double the coupling constant α_t^2 for transverse phonons, to be compared with a constant value of coupling constant employed by Schrieffer et al (1963).

Scalapino et al (1965) have calculated that there may be an anomaly in the effective tunneling density of states of Pb at $T \approx T_c$. This is explained in terms of removal of

an electron from the normal metal and a quasi-particle from the superconducting Pb and creation of a ground state pair in Pb with emission of a phonon. At non-zero temperatures, there are a relatively large number of excited quasi-particles and high density of states at the gap edge in Pb. An electron can be injected from a normal metal into Pb across an insulating layer and can then combine with an excited quasi-particle and form a ground state pair. A phonon is emitted in this process. Because of the high density of states at the gap edge and the requirements of energy conservation, this process is most probable when

$$v + \Delta_o(T) = \omega^{\lambda} \qquad (3.19)$$

where ω^{λ} is a peak in the phonon density of states , $\Delta_o(T)$ is the gap parameter at the gap edge at temperature T and v is the energy of the injected electron. Notice the difference between the mechanisms involved in Eqns. (3.18) and (3.19).

According to Scalapino et al (1965), this recombination process causes a new negative peak in the $\Delta_2(E,T)$, as shown in Fig. (3.5), which is eventually reflected in the effective tunneling density of states. This additional structure, due to recombination, is, however, subject to thermal smearing. They estimate that the maximum observable structure should occur near $T/T_c = 0.95$ around an energy $v = 3.9$ mv.

Figure 3.5

Computed real and imaginary parts of the complex gap function $\Delta = \Delta_1 + i\Delta_2$ as a function of energy. The dashed curves are for T = 0, and the solid curves for a reduced temperature $T/T_c = 0.98$ (after Scalapino et al (1965)).

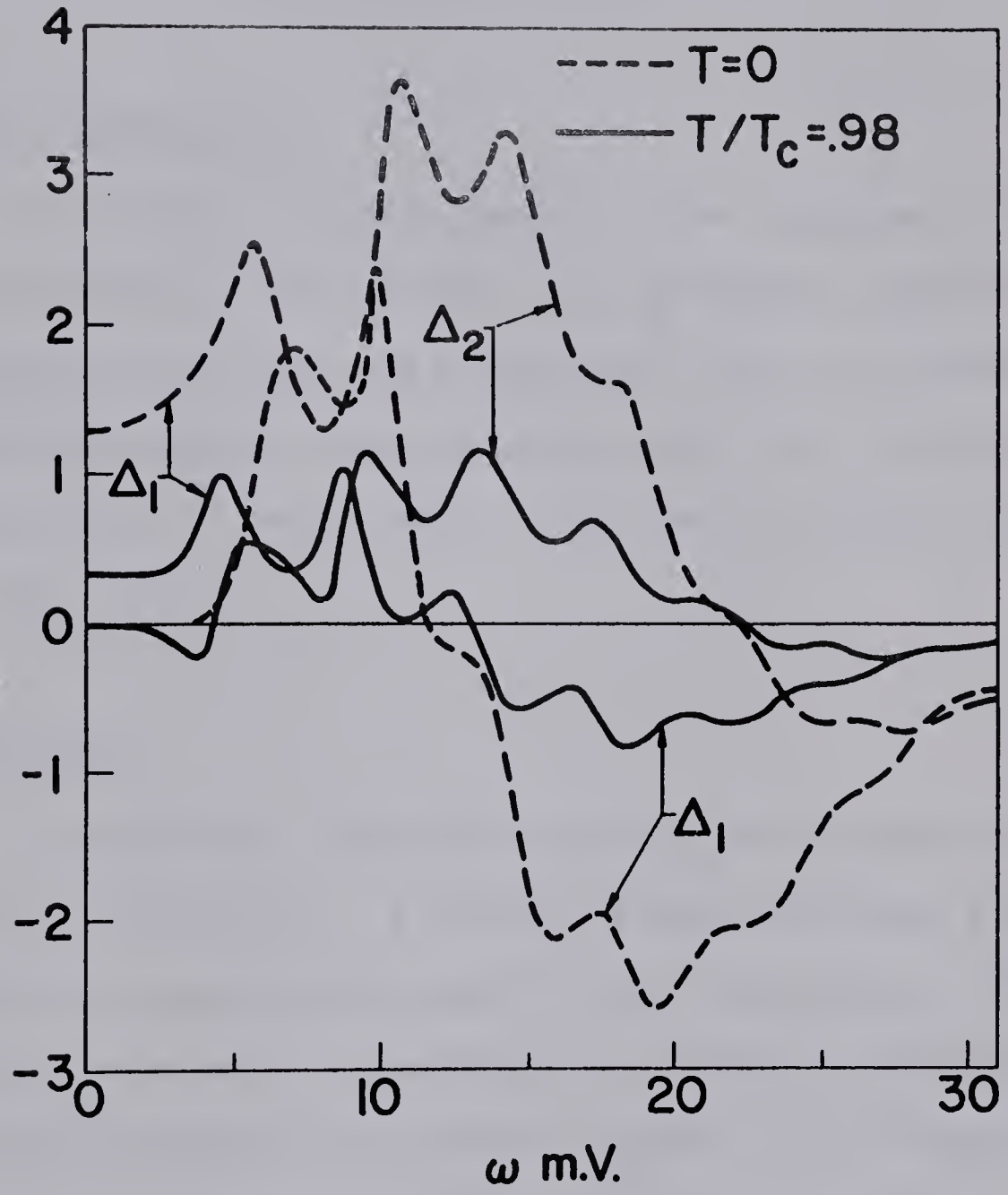
T=0
T/Tc=.98
Δ2
Δ1
Δ1
Δ m.V.
ω m.V.
4
3
2
1
0
-1
-2
-3
0
10
20
30

CHAPTER IV

EXPERIMENTAL METHOD

A. Sample Preparation

The tunnel junction samples were prepared in the manner described by Adler (1963) and by Rogers (1964) except for variation in the oxidation process. Salient features of the sample preparation are reported here. The distinct stages of preparation of a metal/metal oxide/metal sandwich are shown in Fig. (4.1).

(i) Base Layer

99.999% pure aluminum was used as the metal for the base layer in this work. A cleaned glass slide was placed close behind an appropriate mask in the evaporator. The evaporations were made by heating in vacuum a 0.060" diameter tungsten wire carrying an aluminum charge. All evaporations were started at a pressure of 5×10^{-5} mm of mercury or less. The base layer was approximately 1 mm wide and 100 to 500 A^{o} thick.

Aluminum has been most commonly used as the base layer metal because of the ease with which it may be evaporated and oxidized to yield a suitable barrier layer. It also

Figure 4.1

Various stages of sample preparation:

A. A base layer A was vacuum deposited onto a cleaned glass slide.

B. A barrier layer A_xO_y was formed by oxidation.

C. A cover layer B was vacuum deposited across the barrier layer to form a cross strip.

D. Leads were soldered at the ends of the films.

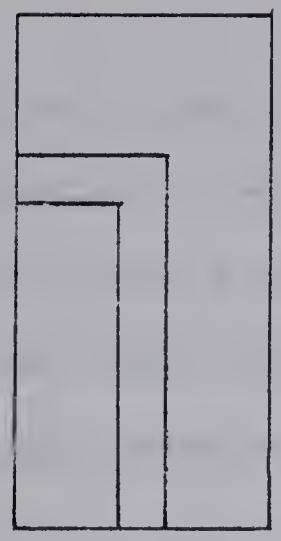

A

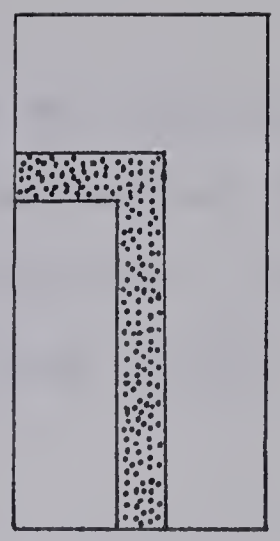

B

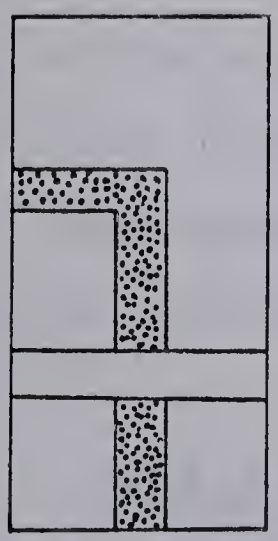

C

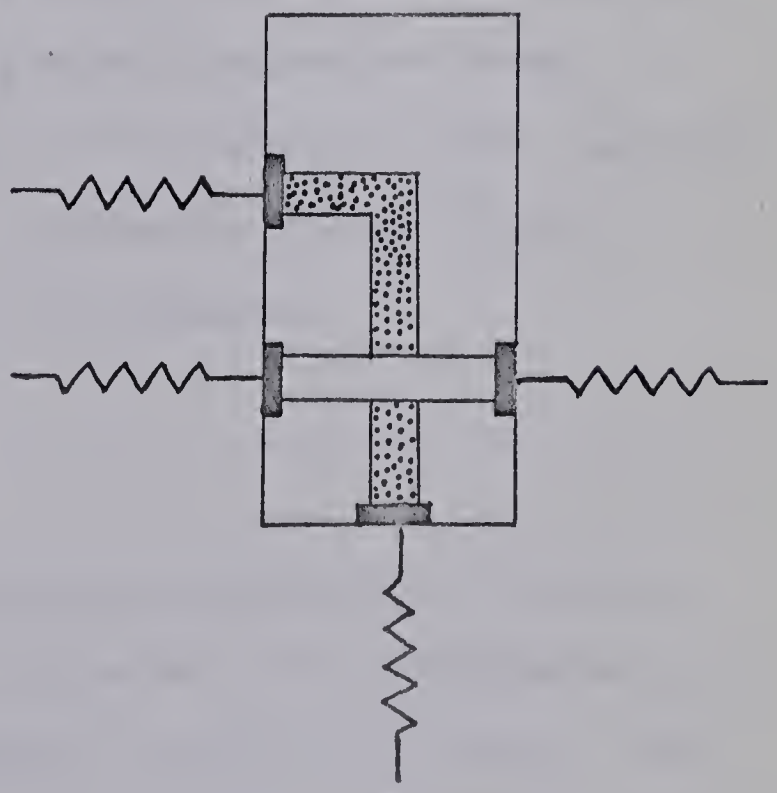

D

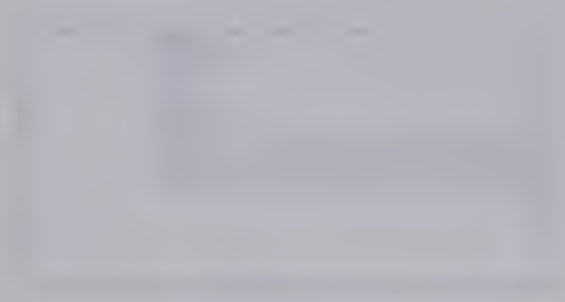

becomes superconducting at low temperatures and thus provides a possible S-S system. Other metals that may be used for base layer preparation are mainly Sn, ~~Mg~~ and Pb (cf. Giaever et al 1962) all of which become superconducting at low enough temperatures.

Magnesium, on the other hand, can provide a normal base layer in a tunnel junction (cf. Rogers 1964). One of the difficulties in evaporation of magnesium was that evaporated magnesium covered the whole glass slide even when the mask was held only 2 mm away from the slide (cf. Adler 1963). Films of magnesium with well defined edges have been evaporated on the glass slides during the course of this work by sudden heating of magnesium ribbons approximately 1.5" x 0.125" x 0.006" in size. A cover slide was mounted on top of the experimental slide to prevent magnesium atoms reflected from various portions of the evaporator from reaching the experimental slide. However, magnesium films of any desired thickness could still not be prepared.

(ii) Barrier Layer

The base layer of aluminum was oxidized in an oven at nearly 200°C. In one specimen reported here, preheated air was blown over the glass slide while it was in the oven. The

temperature of the oven was maintained at nearly 200°C in this case also. The water vapour content of the air near the specimen is possibly higher in the latter case and this seemed to accelerate the oxidation. Oxidation time in all cases was about one minute.

(iii) Cover Layer

A strip of high purity lead was vacuum deposited across the barrier layer. The evaporation was done in vacuum by heating a molybdenum strip carrying a charge of lead.

(iv) Lead Connections

Finally a wire was attached to each of the four ends of these two strips using pure indium solder. Fine copper wires coated with 50:50 lead-tin solder were used for the leads. The coating on these wires becomes superconducting at low temperatures and this reduces the heat input to the specimen. This method of connecting leads after evaporating the cover layer allows the oxidation to be carried out above the melting point of indium.

(v) General Considerations in Sample Preparation

Resistance and capacitance of the tunnel junction were measured with a R-C bridge described by Rogers (1964). The special feature of this bridge is that it cannot subject the tunnel junction to more than 50 mv. Four terminal measurements of the resistance of the tunnel junction were also made. The specimens used in the present work had resistances in the range from 100 to 500 Ω (ohms) measured between the metallic films and from this the barrier layers were estimated to be a few tens of A^{o} thick. The resistance of the evaporated films was always less than 10 Ω.

The thickness of the barrier layers reported by Giaever and Megerle (1961) and by Rogers (1964) depends on a number of variables. The oxidation rate strongly depends on the oxidation temperature and the atmospheric humidity or the residual H_2O vapour in the system. Elevated temperatures and an increase in humidity facilitate oxidation as was well borne out by the present work. The oxidation rate in a confined atmosphere of oxygen at 100 to 400^{o} C was found to be lower than in open air at the same temperature. The effective barrier thickness is also dependent on the nature of the cover layer, evaporation temperature of the cover layer and finally the rate of evaporation of the base layer itself. We have

found during the course of the present work that a tunnel junction with almost any value of resistance could be prepared by suitably controlling these parameters.

The characteristics of the specimens prepared at room temperature generally changed with time. Stable specimens, whose resistance and capacitance remained almost constant at room temperature, were prepared by oxidizing the base layer in an oven. The elevated temperatures in the oven perhaps help in achieving equilibrium surface characteristics of the base and the barrier layers which gave stability to the specimen.

For small voltages v, the current i through the barrier layer was found to be proportional to the applied voltage across it. The current increased approximately exponentially with voltage at higher voltages which is consistent with the results obtained by Fisher and Giaever (1961). Figs. 4.2(a) and (b) show the i:v characteristic of a typical tunnel junction.

The barrier layer does not have a uniform thickness. This is supported by results of Fisher and Giaever (1961) and of this laboratory (cf. Rogers 1964). Measurable strengths of tunneling currents due to dpt processes have also been explained in terms of non-uniform thickness of the barrier layer (cf. Chapter III). A few fine metal bridges piercing the

Figure 4.2

Current-voltage characteristics of a typical tunnel junction at (a) low voltages (after Fisher and Giaever 1961),
(b) higher voltages (after Adler 1963).

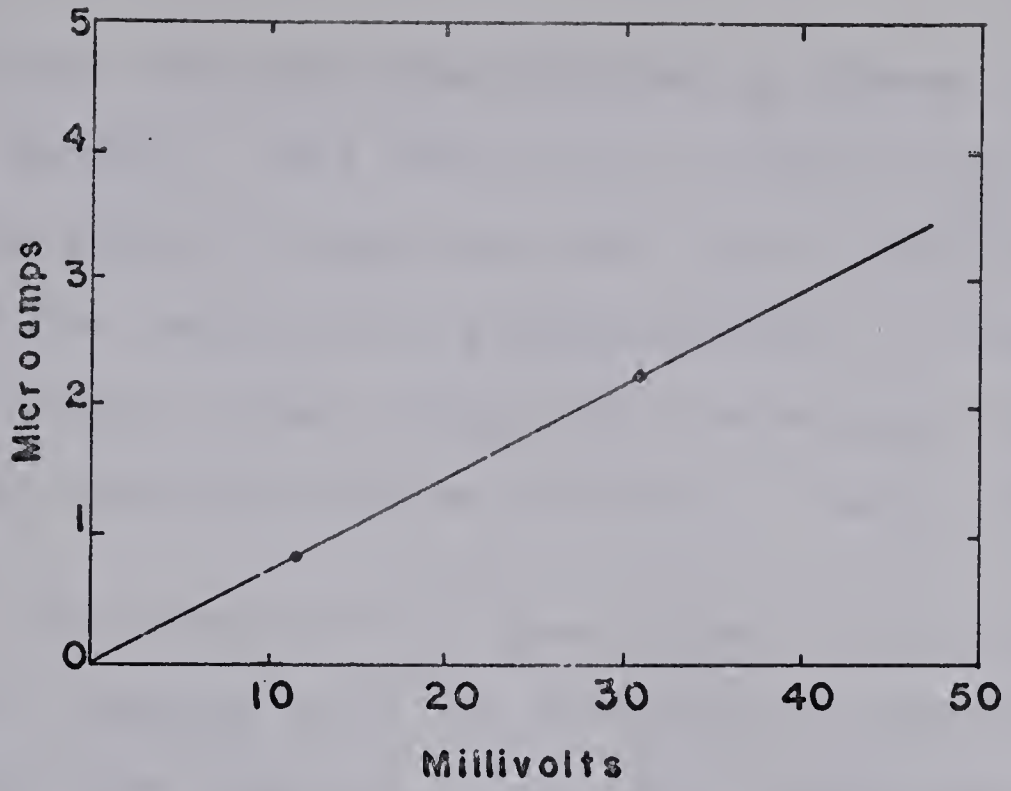
5
4
3
2
1
0
Micro amps
10
20
30
40
50
Millivolts

(a)

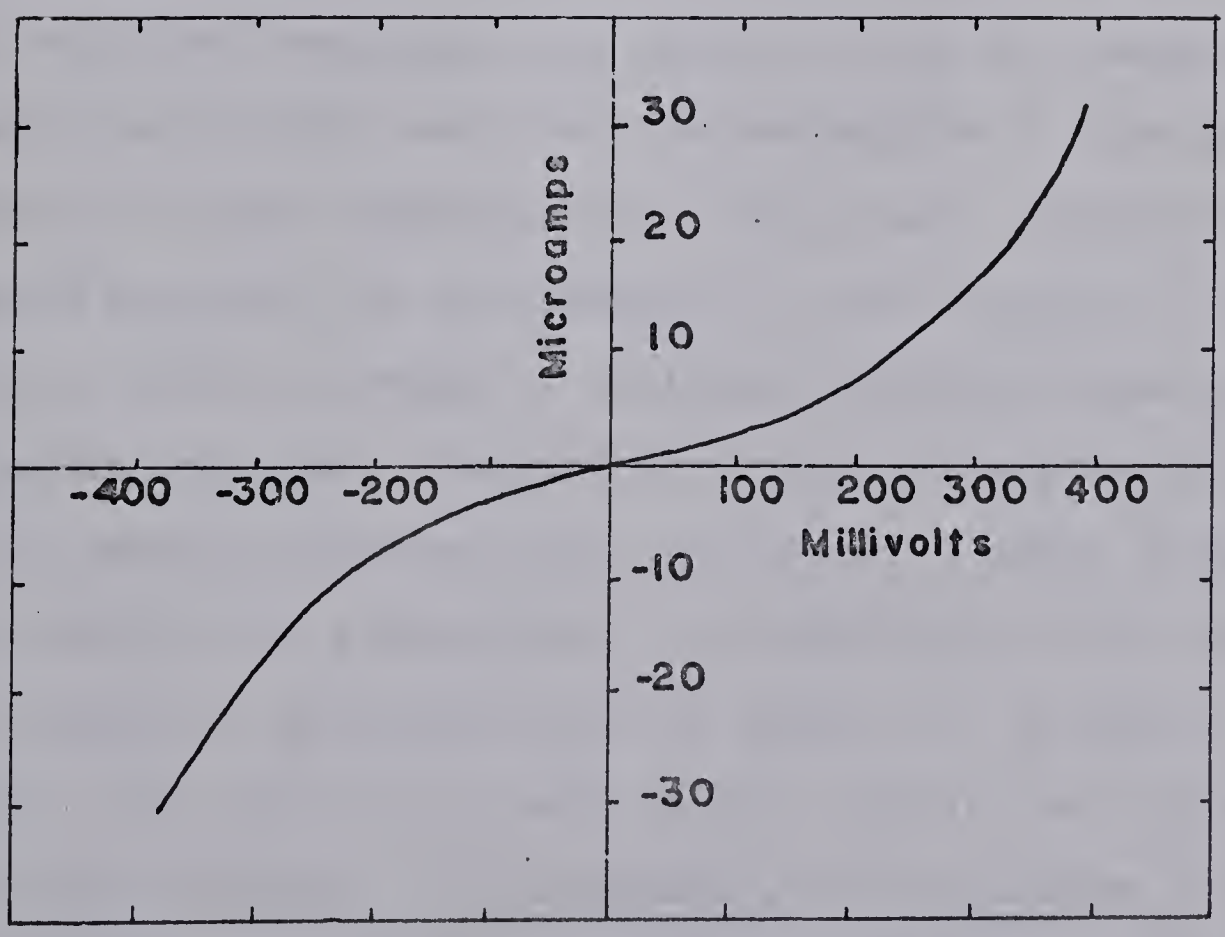
30
20
10
Microamps
-400
-300
-200
100
200
300
400
Millivolts
-10
-20
-30

(b)

barrier layer have also been reported by Giaever (1960) and by other workers. This results in a slight current at voltages well within the gap even when one or both of the metallic layers of the junction are superconducting. A tunnel junction having a number of such bridges will have many discontinuities in its i:v characteristic as observed by Rogers (1964).

The selection of a good tunnel junction was rather difficult. As soon as it was prepared, its resistance and capacitance were measured. Only those stable specimens which had resistance lying in between 100Ω and 500Ω were chosen. A very thin barrier layer corresponding to a resistance less than 100Ω may rupture at low temperatures. The higher limit of the specimen resistance was partly set by our measuring equipment and by the fact that the resistance of the specimen increased at lower temperatures. The primary characteristics of a good specimen are the presence of non-linear i:v characteristic, little increase of resistance with decrease in temperature and sharp transitions from a N-N system to a N-S or a S-S system consistent with the theory. These characteristics confirm the predominance of tunneling current over any other conduction mechanism and the absence of metallic bridges. The latter will particularly obscure any current due to dpt processes. Unfortunately, the existence of these characteristics can be completely confirmed only when the specimen has been cooled to liquid helium temperatures.

Figure 4.3

Schematic of drawing showing the method of specimen mounting and the specimen chamber. The drawing is nearly twice the actual size.

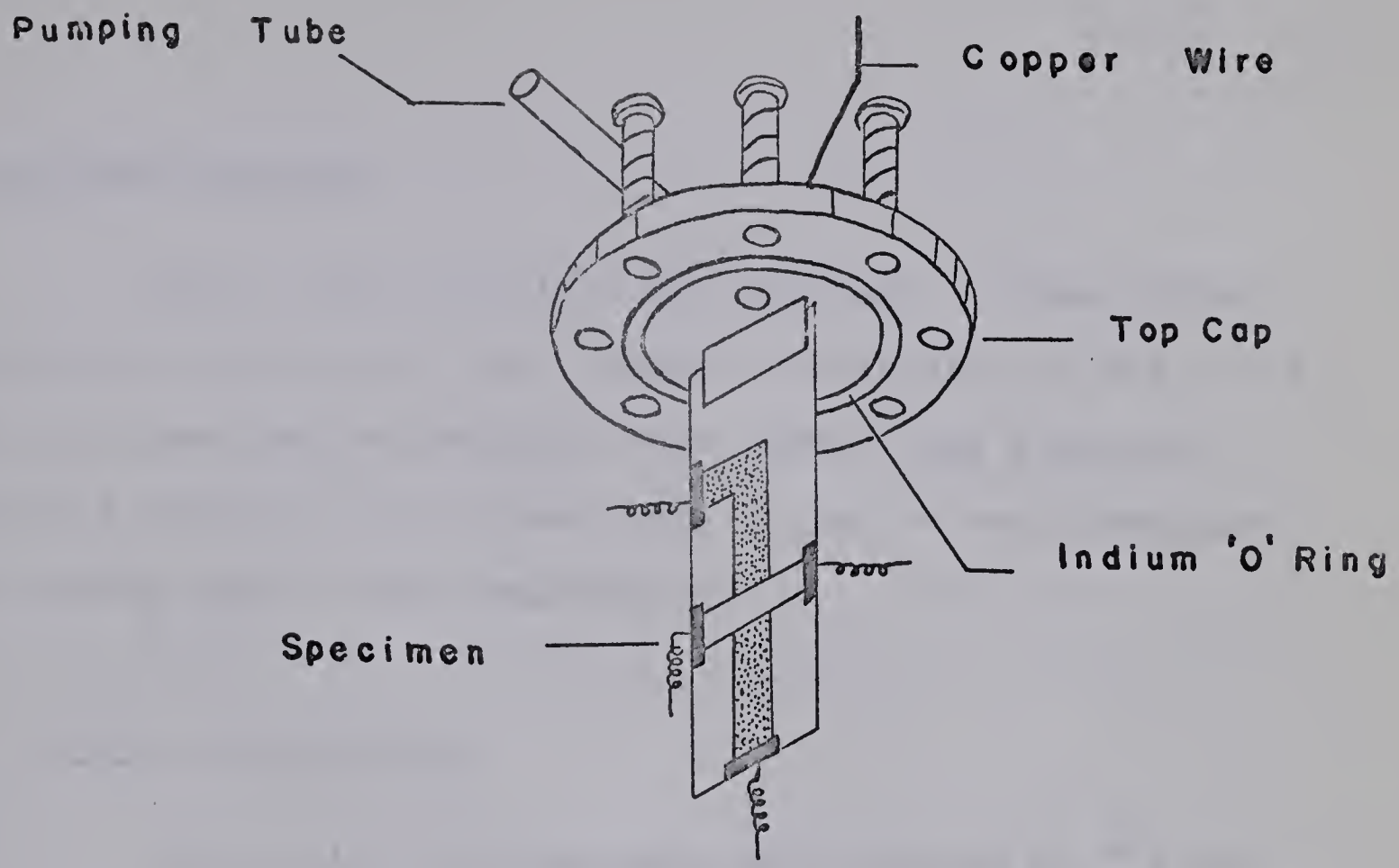
Pumping Tube
Copper Wire
Top Cap
Indium 'O' Ring
Specimen
Kovar Sleeve
Glass
Kovar Tubes

B. Specimen Mounting

After a good specimen was obtained, it was quickly mounted in a small gas tight chamber illustrated in Fig. (4.3). After the specimen was mounted, the chamber was evacuated through a pumping tube and was then filled to one atmosphere with helium gas at room temperature.

C. Cryostat Description

The Al-Al_xO_y-Pb specimens were studied at 7^oK and at approximately 0.3^oK. Hence a He^3 cryostat was necessary for this work. At the lower temperature both the metals of the tunnel junction were superconducting and their energy gaps would be fully developed.

The cryostat has been described in detail by Adler (1963). Fig. (4.4) illustrates the experimental chamber. 0.3^oK is roughly the lowest attainable temperature in this cryostat. Electrical connections to the specimen chamber were made with lead-coated copper wires 0.0025" in diameter. The copper wire and helium in the specimen chamber served as the thermal link between the specimen and the He^3 chamber. A germanium crystal was attached to the He^3 chamber to record the temperature of the specimen.

Figure 4.4

Schematic of drawing showing the experimental chamber of the cryostat.

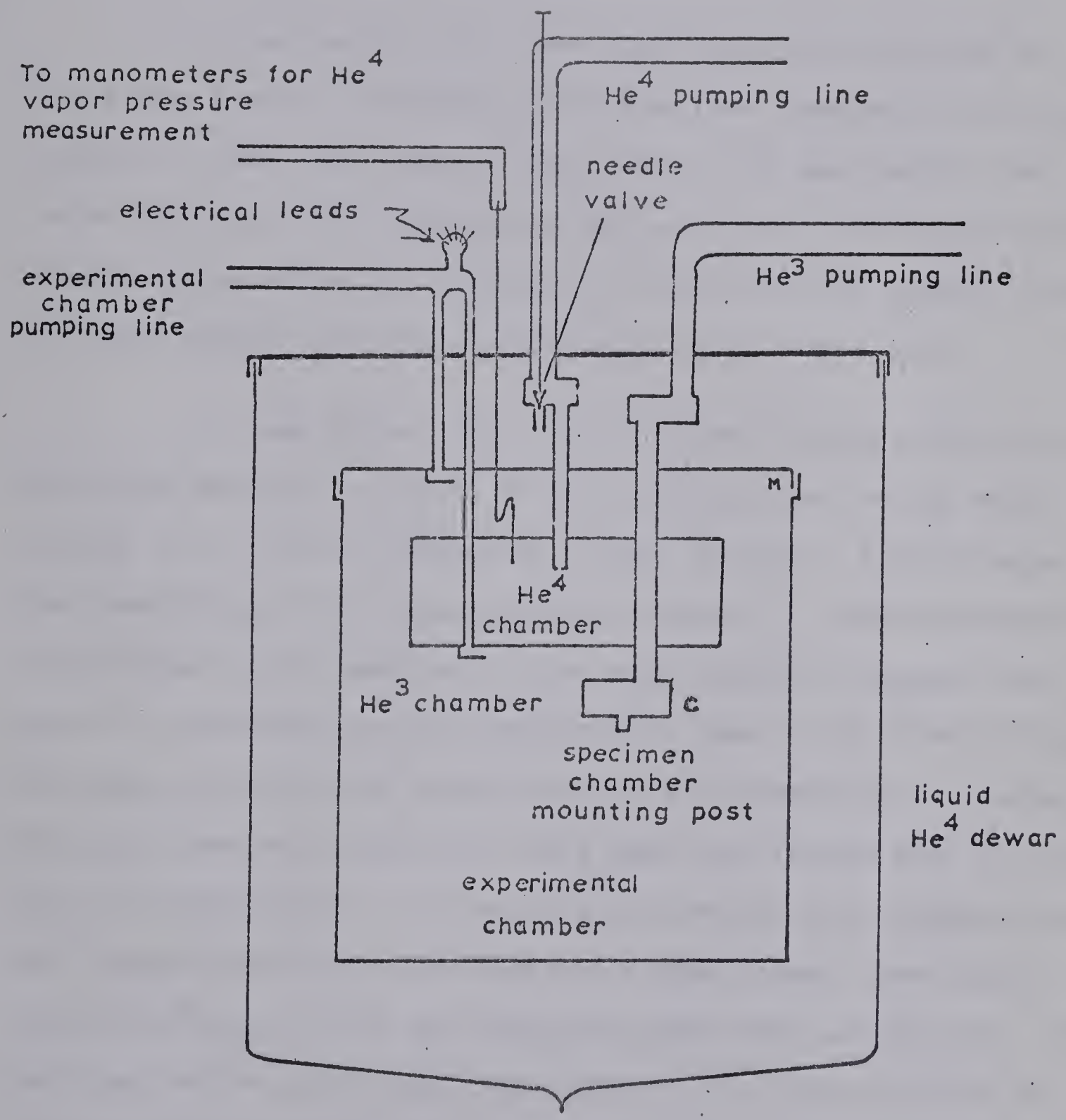
To manometers for He4 vapor pressure measurement
He4 pumping line
needle valve
electrical leads
He3 pumping line
experimental chamber pumping line
M
He4 chamber
He3 chamber
C
specimen chamber mounting post
liquid He4 dewar
experimental chamber

(i) Operating Procedure of the Cryostat

In an actual run, the outer can was soldered to the plate M after connecting the specimen chamber to the He^3 chamber C (cf. Fig. 4.4). This joint at M was tested for leaks both at room temperature and at liquid air temperature. Standard procedure for cooling to liquid helium temperatures was used except for the following special precaution.

It was noted that the pressure reading obtained in the room temperature part of the pumping line to the outer can is a very poor indication of the amount of the exchange gas remaining in the experimental chamber. Large amounts of helium gas still remained in the experimental chamber even when the pressure in the pumping line was 5×10^{-6} mm of Hg. This gas could not be pumped out of the experimental chamber during a period of several hours when the latter was at liquid helium temperatures. It provides a thermal link between the He^3 chamber and the outer can and temperatures lower than about $0.6^{\circ}K$ could not be obtained under such conditions. The helium leak detector was connected to the vacuum system for the experimental chamber to serve as a monitor for the amount of helium gas present in the experimental chamber. The temperature inside the experimental chamber was then allowed to rise to nearly $20^{\circ}K$ with very little liquid helium in the outer dewar. Thereafter the leak detector reading fell by a factor

of nearly 10^3 in a period of nearly six hours. The outer dewar was filled with liquid helium only when the exchange gas was thus completely pumped out. Liquid helium temperatures could be reached without admitting exchange gas to the experimental chamber at all below liquid air temperatures. However, it was found that more time was required to reach liquid helium temperatures by this method.

The temperatures between $0.3^{\circ}K$ and 7° K were obtained with the help of the heater mounted on the He^3 chamber and partly by regulating the pumping speed in the He^3 system.

D. Temperature Calibration

The temperatures reported in this work are those of the He^3 chamber which was in thermal equilibrium with the specimen. The temperature of the He^3 chamber was inferred from resistance measurements of a Ge crystal mounted on the He^3 chamber. Four terminal resistance measurements of this crystal were achieved by using an isolating potential comparator of the type described by Dauphinee (1953). It is essential to obtain a calibration curve for this thermometer. Wires of high purity lead, aluminum and cadmium were wound on a thin copper cylinder which was mounted on the He^3 chamber. The resistance of the Ge thermometer was measured at the transition

temperatures of these metals. The transitions from the normal to the superconducting state for these metals were determined by using a four terminal resistance measurement with a circuit described by Rogers (1962). A fourth calibration point was obtained by admitting exchange gas to the experimental chamber and opening the needle valve to connect the He^4 chamber to helium gas at atmospheric pressure. The vapour pressure of the boiling liquid helium was noted from the mercury manometer.

E. Measurement of i:v Characteristics

The i:v characteristics of the tunnel junctions were measured with a curve tracer described by Rogers, Adler and Woods (1964) which permits sensitive four terminal resistance measurements. $(di/dv)_s / (di/dv)_n$ can be calculated at different voltages v across the specimen from these measurements. Calculations were carried out with IBM 7040 computer.

CHAPTER V

EXPERIMENTAL RESULTS AND DISCUSSION

A. Temperature Measurements

Two lead specimens with Al as the base layer were studied. Accurate measurement of the temperature was essential for this work as we were looking for the additional peak in the density of states in lead at temperatures close to its transition temperature T_c. The transition temperatures of Pb, viz, 7.193°K (cf. Franck and Martin, 1961), Al, viz, 1.196°K (cf. Cochran and Mapother, 1958) and Cd, viz, 0.52°K (Martin, 1961) were used to calibrate a germanium resistance thermometer. Another calibration point was obtained at the boiling point of the liquid helium.

The above-mentioned calibration points were successively fitted to the following interpolation equations relating the thermometer resistance and its temperature. These equations are respectively due to Clement-Quinnell (1952) and Clement (cf. White 1957).

$$T^{-1} = a(\ell nR)^{-1} + b + c\ \ell nR \qquad (5.1)$$

and

$$T = A\ \log_{10}R/(\log_{10}R - B)^2 \quad . \qquad (5.2)$$

The resistance temperature curves obtained through these equations are shown in the Fig. (5.1). A reversal of the curve obtained from Eqn. (5.1) at higher temperatures is similar to that reported by Rogers (1964) for a 220 ohms 'speer' carbon resistor. It indicates that Eqn. (5.1) is not suited particularly to these thermometer materials over this range of temperature.

From these four calibration points, three (or two) were used in finding the unknowns in Eqn. (5.1) (or Eqn. (5.2)) and the remaining one was used to check the accuracy of the calculated temperature at the corresponding resistance of the germanium thermometer. We also had access to the resistance-temperature curve* obtained by Dr. Franck for a similar germanium thermometer which was calibrated by vapour pressure measurements over boiling He^3 and He^4 between 3.88°K and 0.61°K. Using this calibration curve the error could be determined in any temperature calculated with one of the interpolation equations. The temperatures calculated from Eqns. (5.1) and (5.2) were found to be much different from the correct temperatures.

A quadratic equation

$$\log_{10} R = a + \frac{b}{T} + \frac{c}{T^2} \qquad (5.3)$$

---

*It is a pleasure to acknowledge my gratitude to Dr. J.P. Franck for providing me this calibration curve for the germanium thermometer.

Figure 5.1

Resistance temperature calibration curve for the germanium thermometer using

A. Clement - Quinnell Equation.

B. Clement Equation.

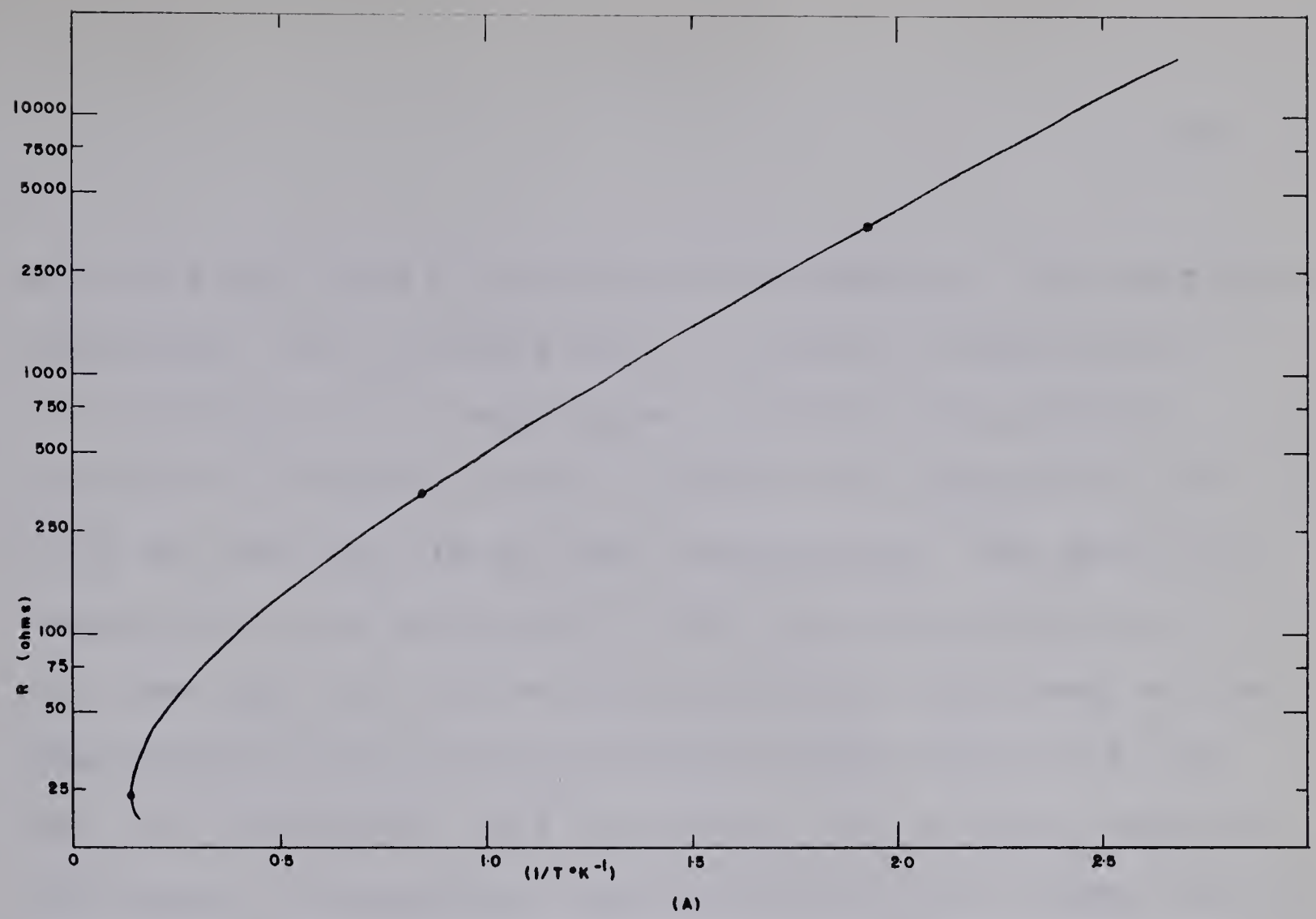
10000
7500
5000
2500
1000
750
500
250
100
75
50
25
R (ohms)
0
0·5
1·0
1·5
2·0
2·5
(1/T °K⁻¹)
(A)
• Calibration points

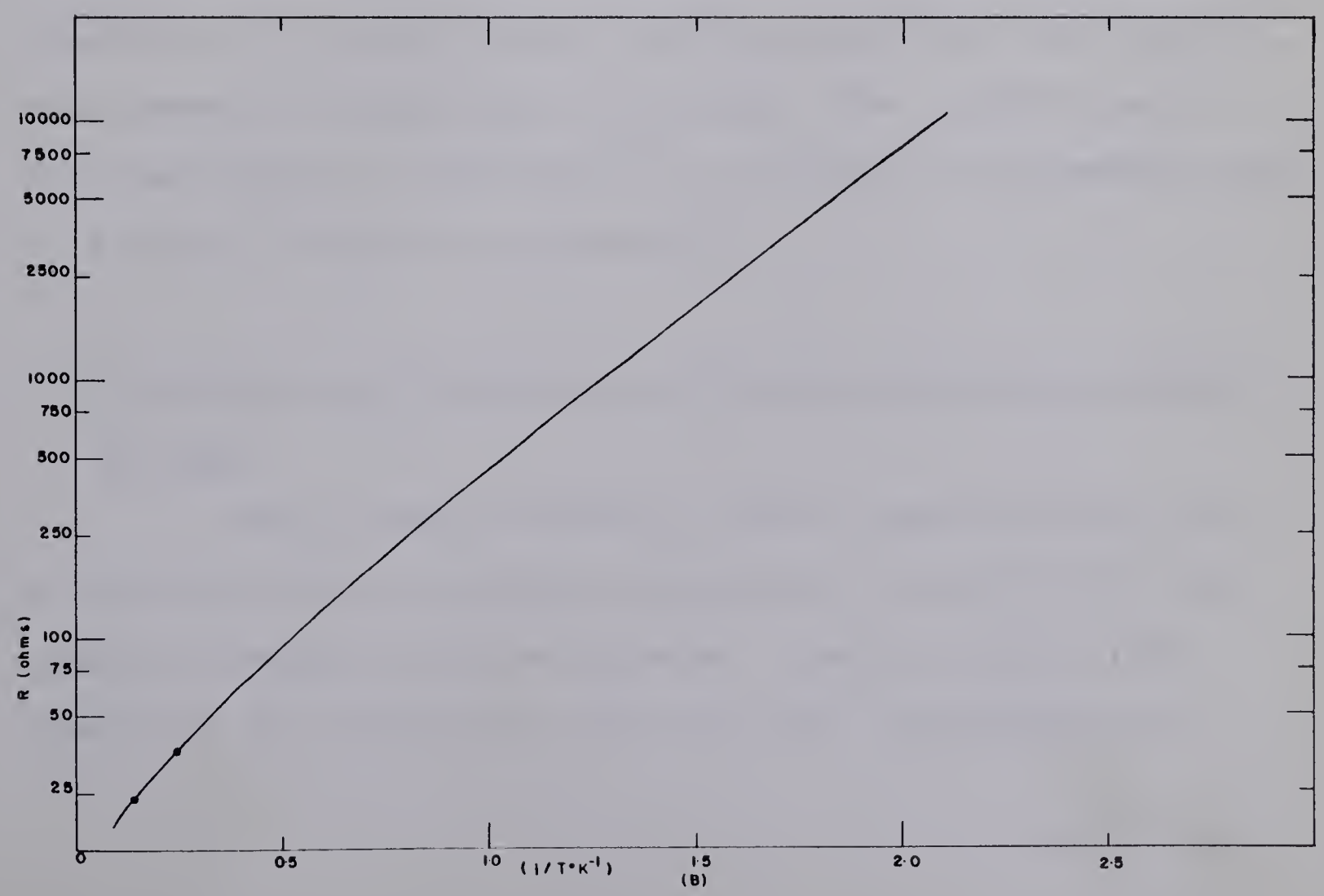
10000
7500
5000
2500
1000
750
500
250
100
75
50
25
R (ohms)
0
0·5
1·0
1·5
2·0
2·5
(1/T°K⁻¹)
(B)

was tried and found to be much more successful. The resistance-temperature curve obtained with it is shown in Fig. (5.2). The uncertainty in a temperature calculated through this equation is estimated to be ± 0.05°K in the range from 7.2°K to 2.5°K and was about 1% at lower temperatures. The error in a temperature close to any one of the calibration points is much less than this maximum uncertainty and since most of the observations in the present work were taken close to T_c for lead, the accuracy of this calibration was certainly adequate. The change in thermometer characteristics after thermal cycling between room and liquid helium temperatures noted by Rogers (1964) in case of the 'speer' resistor was observed not to occur with the germanium element, but the calibration was checked at the liquid helium boiling point after each set of measurements to guard against changes. The current used in the measurement of resistance of the germanium thermometer was 2 μa above 1°K and 0.5 μa below 1°K.

B. Recombination Effects on the Tunneling Density of States in Lead

Lead, being a strongly coupled superconductor with a relatively high transition temperature, is one of the most studied elements in tunneling work. Giaever (1960 a) and Giaever et al (1962) were first to study the variation of

Figure 5.2

Resistance temperature calibration curve for the germanium thermometer using Eqn. (5.3).

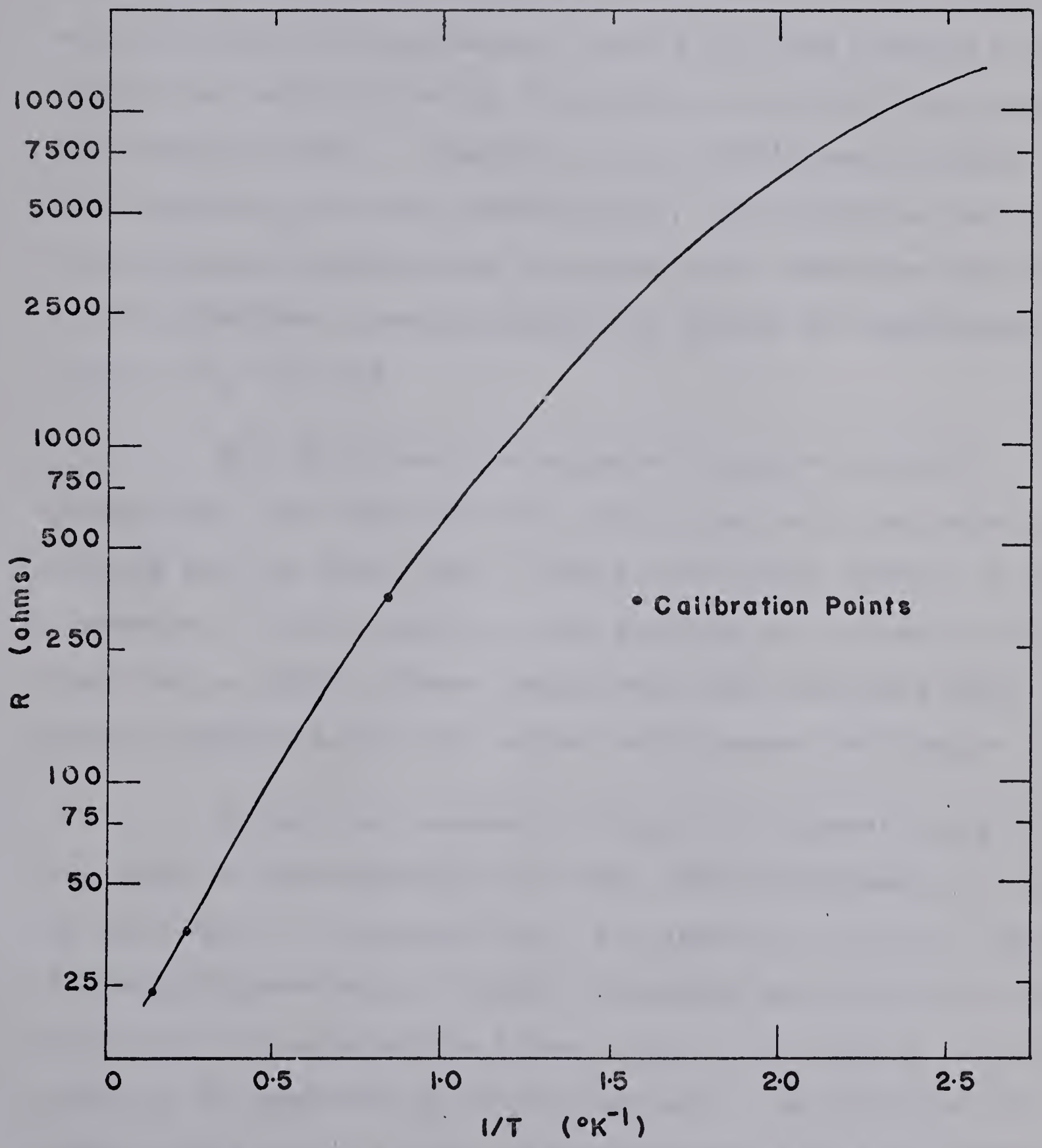
10000
7500
5000
2500
1000
750
500
250
100
75
50
25
R (ohms)
• Calibration Points
0
0·5
1·0
1·5
2·0
2·5
1/T (°K⁻¹)

normalized dynamic conductance with voltage across the specimen as well as the phonon effects in lead. Rowell et al (1963) reported detailed experimental results for lead along with the theoretical explanations by Schrieffer et al (1963) and Scalapino and Anderson (1964). Scalapino et al (1965) have extended these calculations to non-zero temperatures. According to their calculations, recombination processes make themselves apparent in the effective tunneling density of states at temperatures close to T_c for lead.

Fig. (5.3) shows the enlarged traces of two Δv:v photographs, one taken when the cover layer metal was superconducting and the other when it was in the normal state. Δv is a measure of non-linearity of the specimen at voltage v (cf. Rogers et al 1964). These traces have been projected onto graphs prepared to fit the actual oscilloscope calibration.

One of the fundamental things of interest to us is the value of the energy gap in lead. Fig. (5.4) shows the trace of the actual i-v characteristic for specimen Pb-46 at $0.34^{\circ}K$. Following Giaever et al (1962), the energy gap value is determined by extrapolating the linear part of the jump in the i-v curve of the specimen to the voltage axis. As explained on pages 22 and 23, AB in Fig. (5.4) represents $2(\Delta_1 + \Delta_2)$ where Δ_1 and Δ_2 are the energy gaps in the two superconductors forming the specimen. The negative resistance region in the i-v

Figure 5.3

Enlarged graphs from photographs of $\Delta v:v$ characteristics for

(a) a N-N system

(b) a S-S system

over the same voltage range across the specimen.

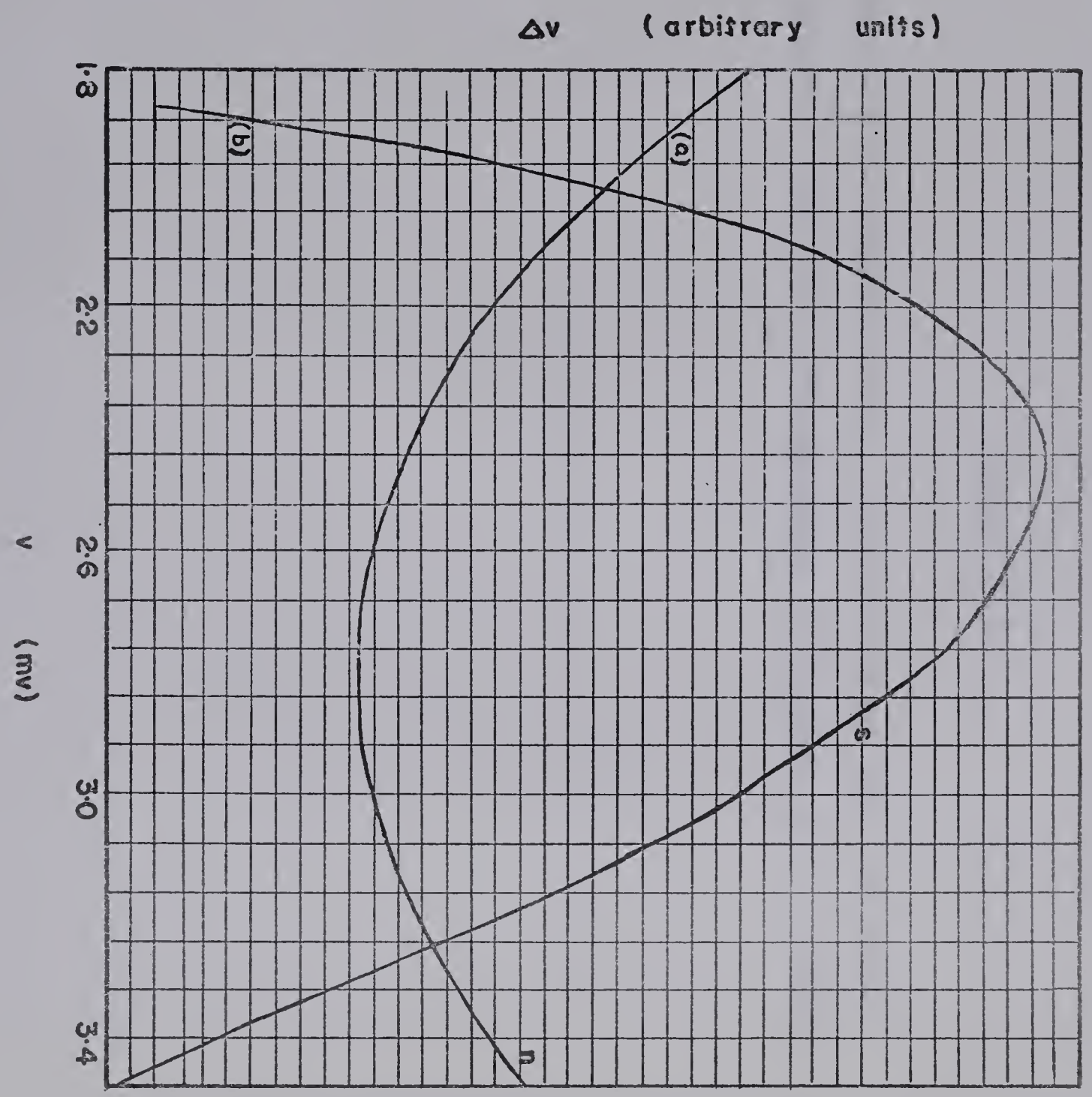
Δv (arbitrary units)
V (mv)
1·8
2·2
2·6
3·0
3·4
(b)
(a)
s
n

Figure 5.4

Graph of i-v characteristic at the energy gap for Pb-46 projected from the corresponding photograph at T = 0.34°K.

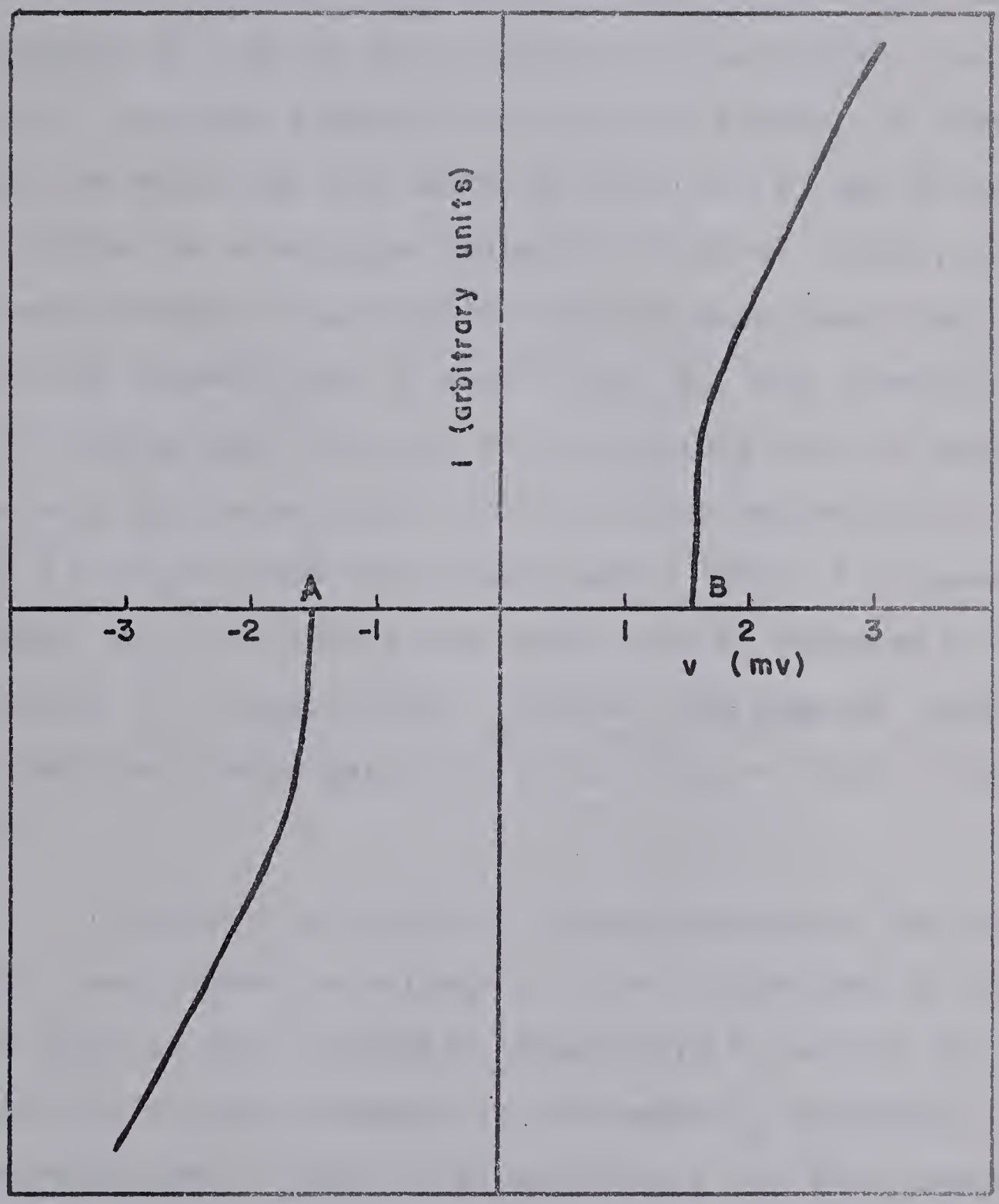
I (arbitrary units)
A
B
-3
-2
-1
1
2
3
v (mv)

characteristic of the specimen is not apparent in this curve due to the current scale chosen here. Rogers (1964) found the value of $2\Delta(0)$ for Al to be (0.42 ± 0.02) mv in this laboratory as compared to 0.40 mv due to Giaever et al (1962). As our method of specimen preparation was quite similar to that of Rogers, we shall use the value of $2\Delta(0)$ for Al due to Rogers. This yields the energy gap value $2\Delta = 2.68$ mv for Pb. As this work was carried out at $0.34^{\circ}K$ which is much less than the transition temperatures of both Pb and Al, the correction to get the energy gap value for Pb at absolute zero is negligible. The energy gap value $2\Delta(0)$ for Pb is thus estimated to be (2.68 ± 0.06) mv from the present work. This is in good agreement with the energy gap values for Pb reported in the literature (cf. Rogers 1964). Giaever and Megerle (1961) had found the energy gap in Pb to be $2\Delta_{Pb} = (2.68 \pm 0.06)$ mv at $1^{\circ}K$.

In order to carry out investigations of the normalized dynamic conductance vs. voltage for the Pb specimen at temperatures close to the transition temperature T_c of the thin cover film of Pb, it was necessary to determine T_c accurately. Fig.(5.5) illustrates some of the i:v presentations for Pb-47 specimen at different temperatures in the neighbourhood of T_c. We have already seen that the i-v characteristic of a N-N system is a straight line and that of a N-S or a S-S system has a flat region at the origin (cf. Fig. (3.1)) if the energy gap in at

Figure 5.5

Graphs of i-v characteristics projected from the photographs around zero voltage for

A. $T = 6.41^{\circ}K.$

B. $T = 6.23^{\circ}K.$

C. $T = 6.09^{\circ}K.$

D. $T = 5.78^{\circ}K.$

Both i and v are in arbitrary units.

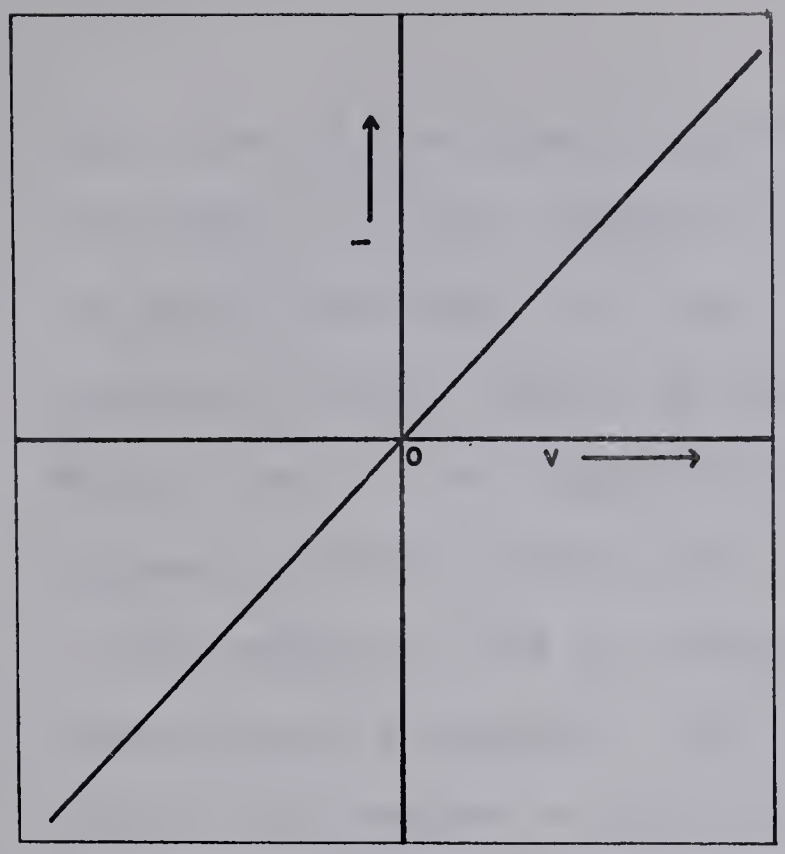

A

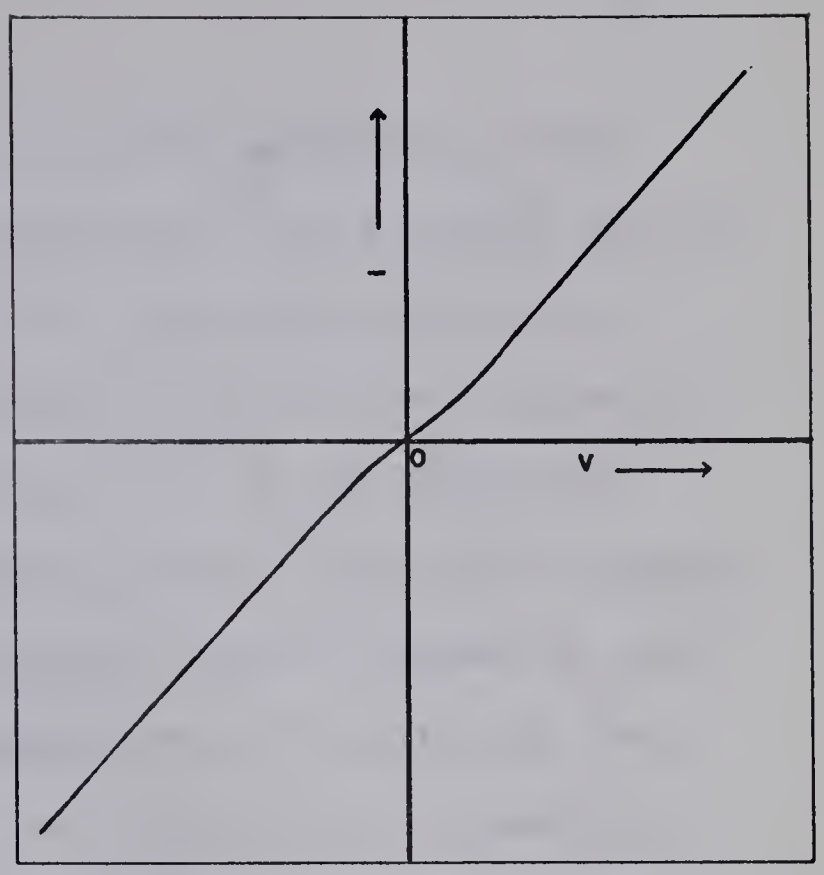

B

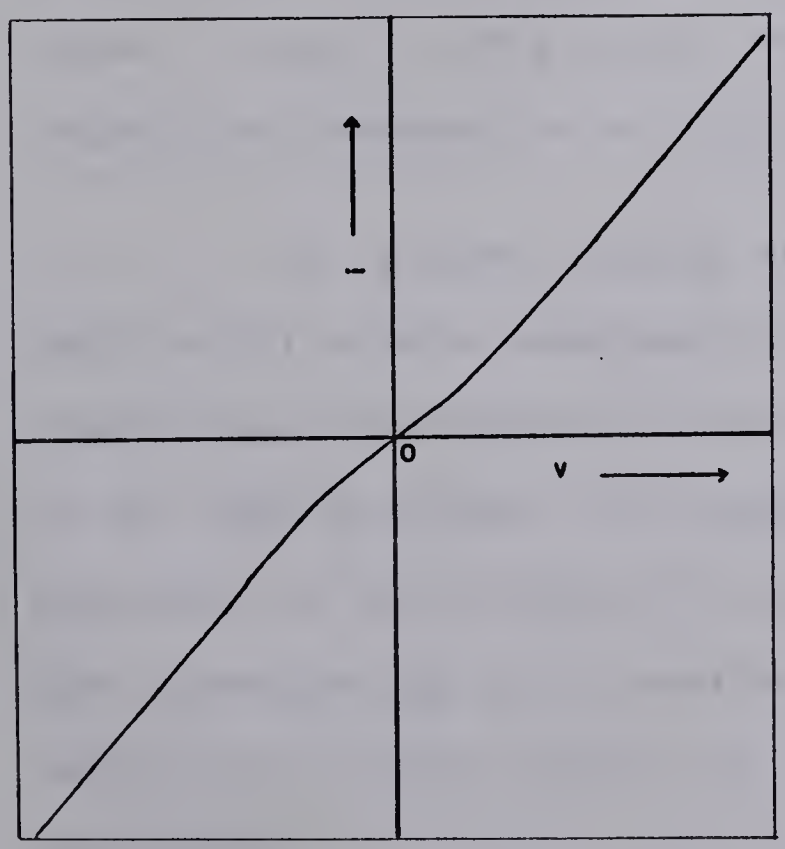

C

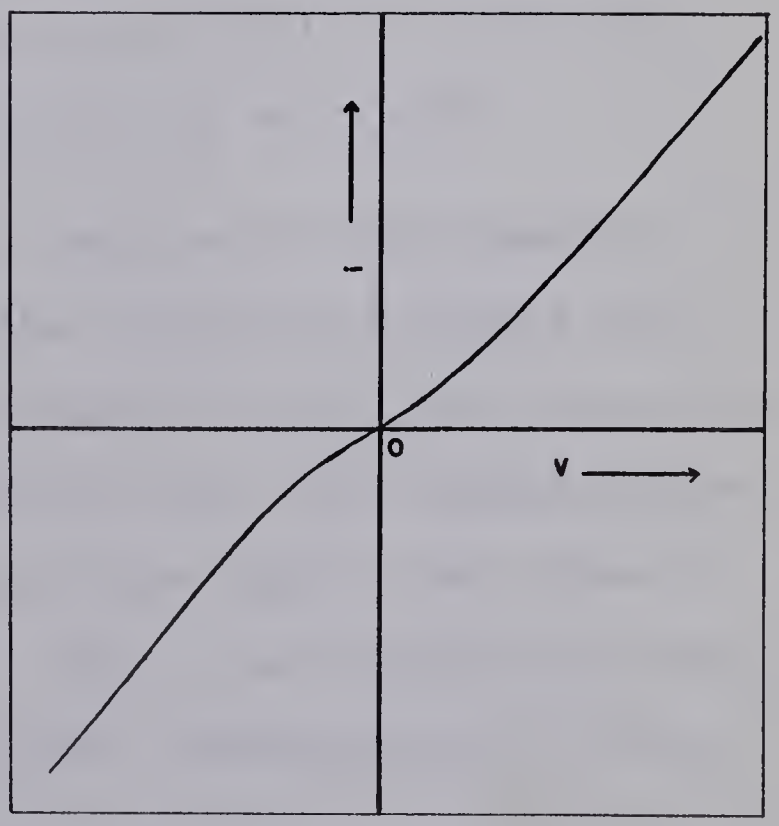

D

least one of the layers constituting the specimen is well developed. At the transition temperature, this energy gap is not fully developed (cf. Fig. (2.2)) and there is also a relatively large number of quasi-particles excited above the Fermi level in the superconducting layer of the specimen. Because of these two factors, only a short flat region appears at the origin in the i-v characteristic and it grows as the temperature is lowered. The appearance of the kink at the origin is, however, a definite indication of the transition of at least one of the films of the specimen from normal to superconducting state. Thus in Fig. (5.5),curve A shows a N- N system and curve B shows that the Pb film has become superconducting (obviously there is no question of superconductivity of the Al film at this temperature). The flat portion at the origin gets larger at lower temperatures as shown in curves C and D in Fig. (5.5) . From these results we find the transition temperature of this Pb film to be $6.32^{o}K$.

It is worth noting that results for this specimen and for all others observed in this laboratory indicate that transition temperatures of thin films of Pb are lower than that of the bulk material. In contrast to this, the transition temperatures of thin films of Al and In are higher than those of the corresponding bulk material. This is an interesting result and it will be the subject of further investigations in this laboratory.

Figs. (5.6 a,b) and (5.7 a) illustrate the σ:v characteristics for the Pb specimen Pb-47 at three different temperatures. The σ:v curve at a reduced temperature $T/T_c = 0.95$ as calculated by Scalapino et al (1965) is shown in Fig. (5.7 b) for comparison. The agreement between the theoretical and the experimentally observed curves is remarkable. As expected from their calculations, structure due to recombination effects is most evident in the energy region near E = 3.9 mv (cf. Chapter III). Further the flat region between the two peaks in the σ:v curves gets shorter as the temperature decreases. This can also be explained qualitatively. As the temperature is lowered, there are fewer quasi-particles excited above the energy gap. The probability of recombination of a tunneled electron with an excited quasi-particle to emit a phonon and form a ground state pair will then obviously be reduced. As the recombination rate decreases, the σ:v curve will gradually return to its usual shape. No definite explanation for the slight difference between the observed and calculated values for the maximum value of σ at the gap edge could be found. This difference was present in both the specimens Pb-46 and Pb-47. It may be due to inhomogeneity and thinness of the Pb film.

Figure 5.6

Normalized dynamic conductance σ vs. voltage v across the specimen Pb-47 at $T \approx T_c$.

(a) $T/T_c = 0.89$.

(b) $T/T_c = 0.96$.

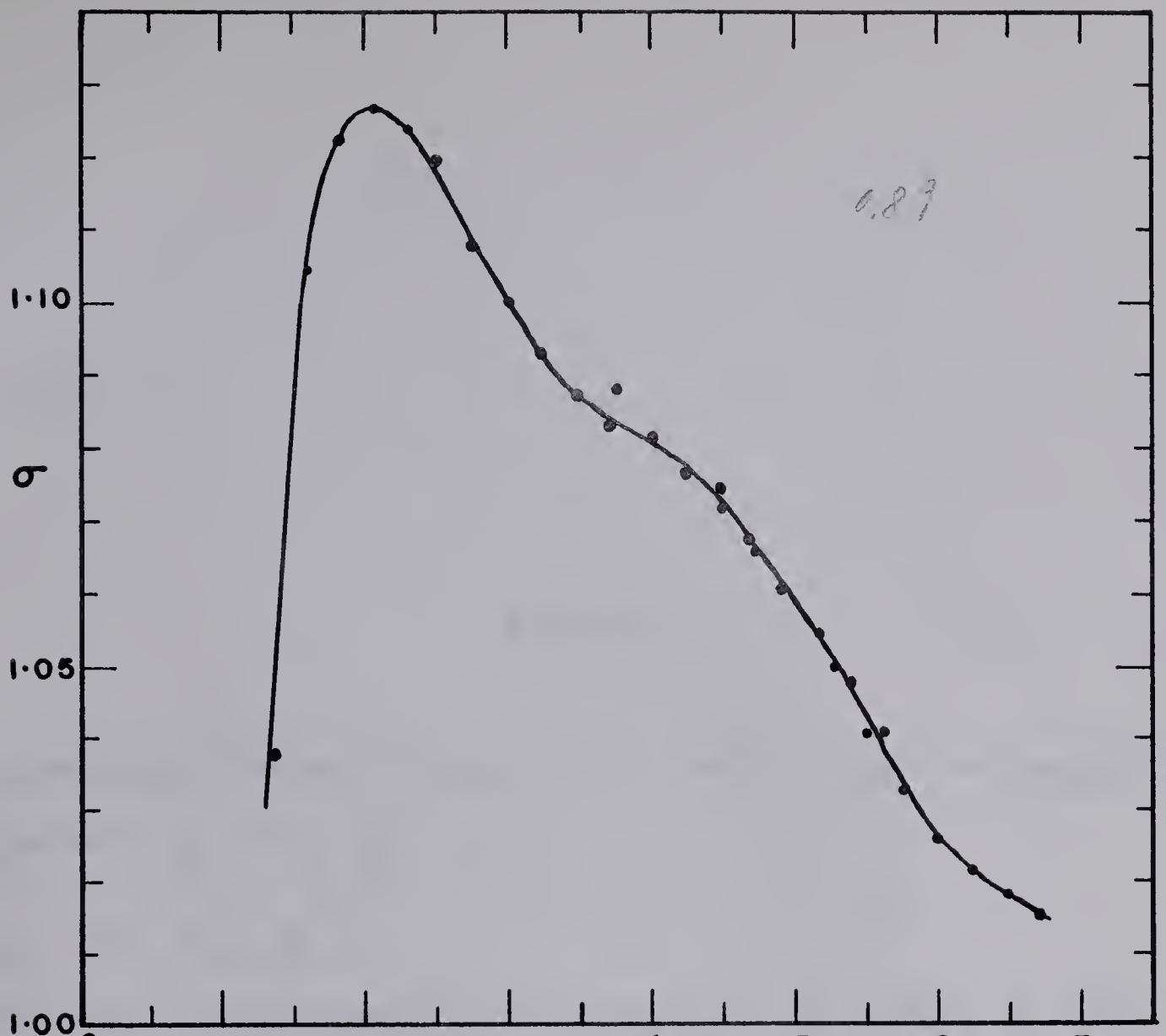

(a)

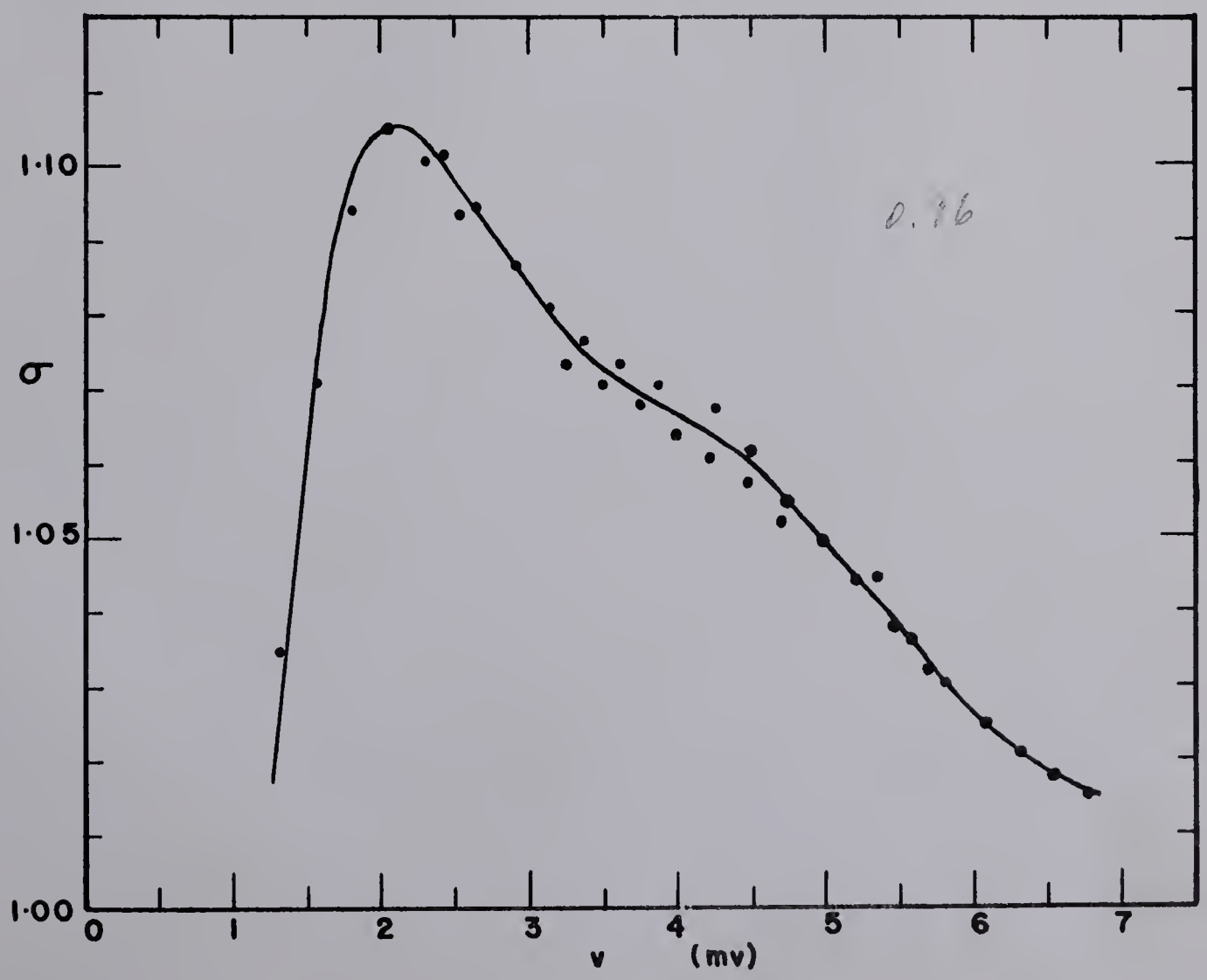

(b)

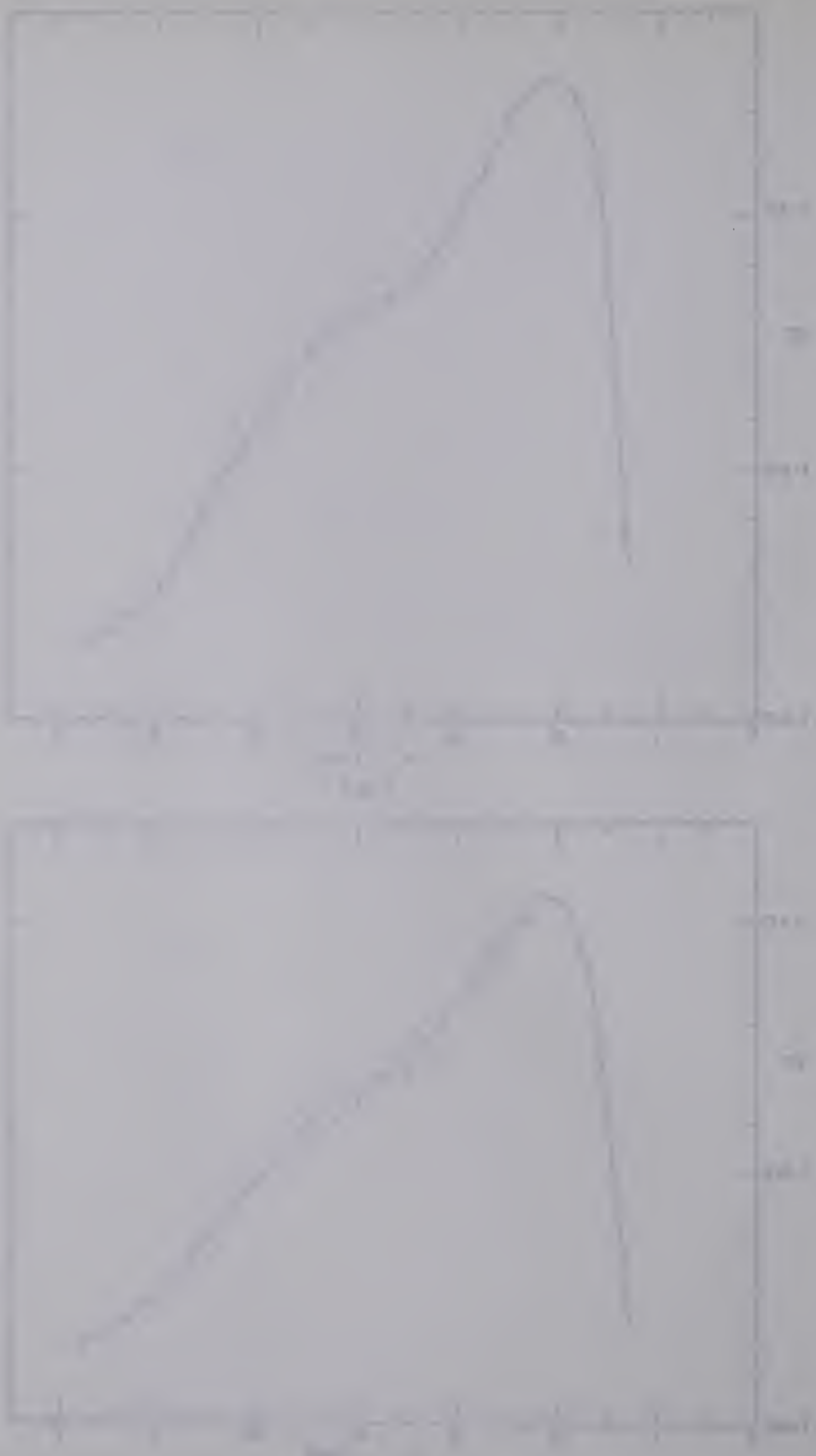

Figure 5.7

Normalized dynamic conductance σ vs. voltage v across the specimen Pb-47 at $T \tilde{\approx} T_c$.

(a) $T/T_c \approx 0.98$.

(b)A. Calculated curve by Scalapino et al (1965) at $T/T_c = 0.95$.

B. Observed results for Pb-46 at $T/T_c = 0.97$.

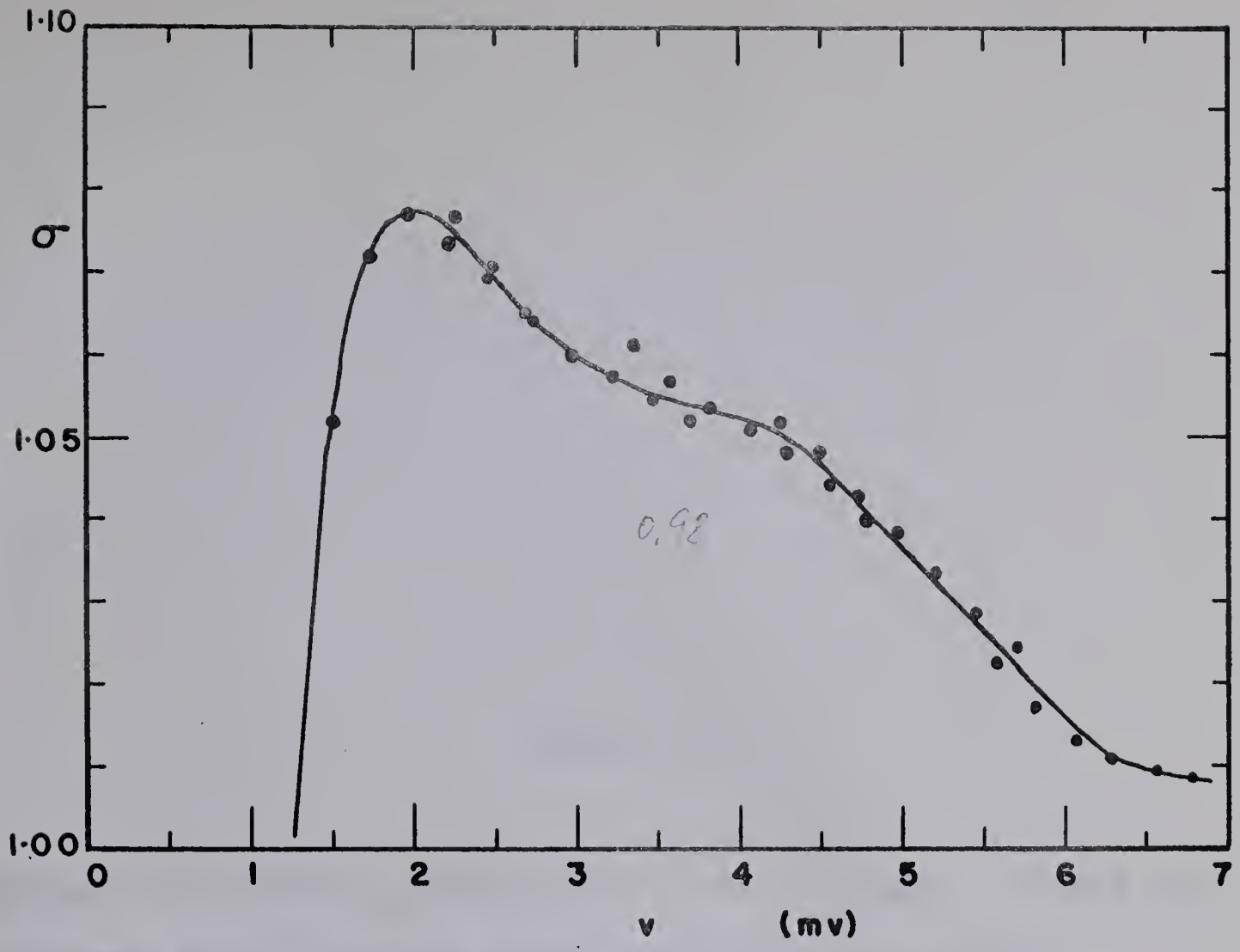

(a)

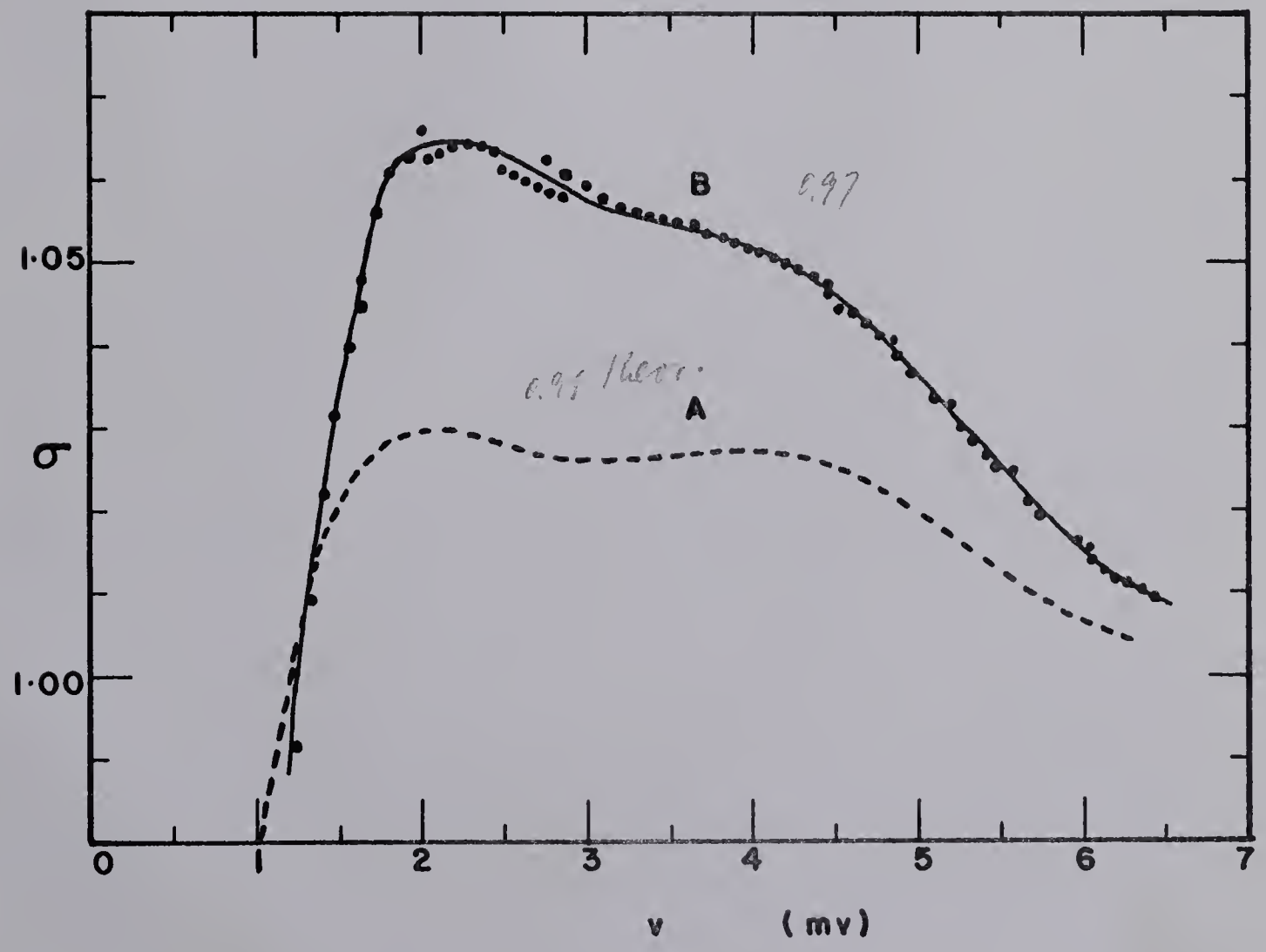

(b)

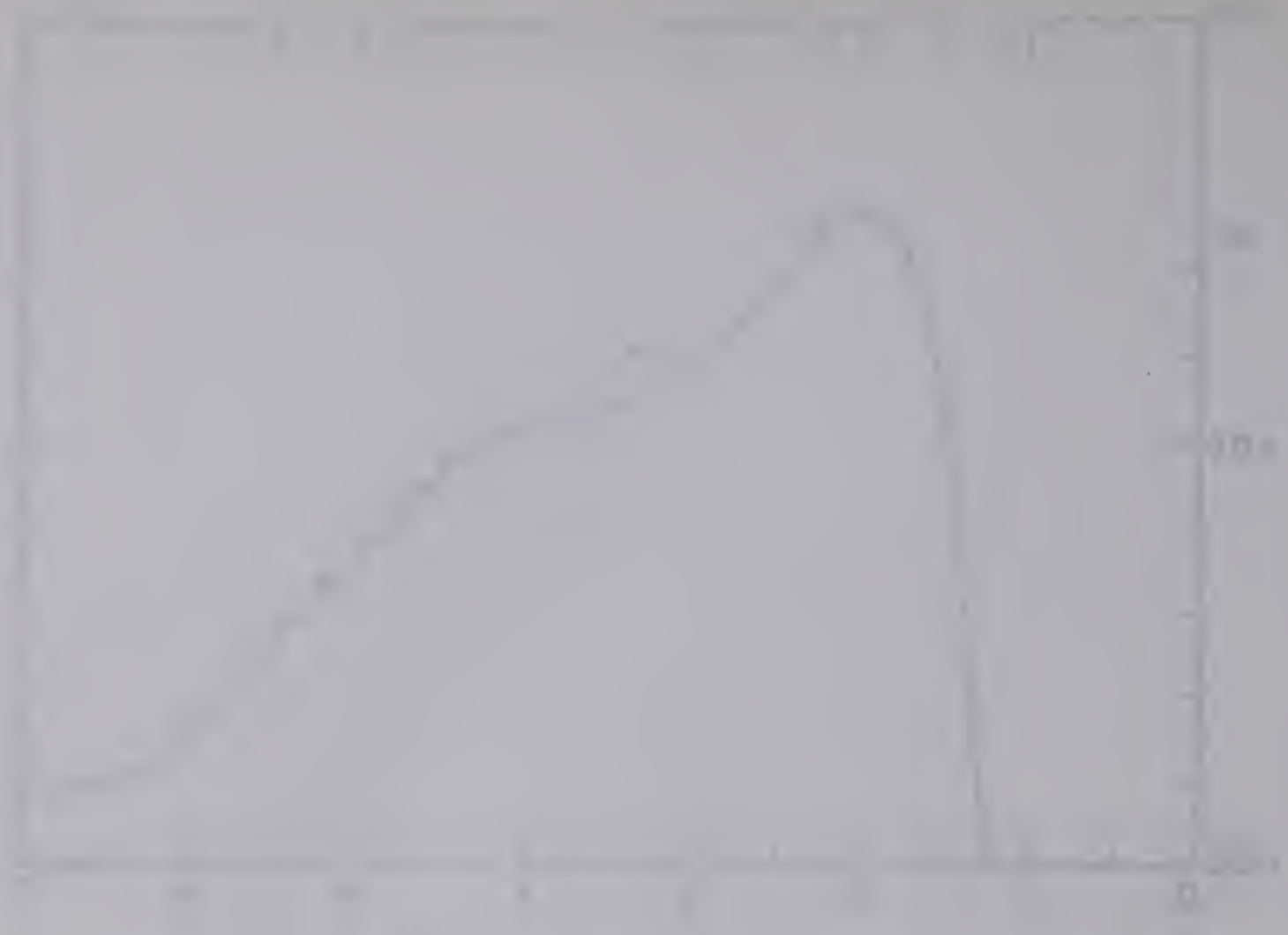

Figure 5.8

Normalized dynamic conductance σ vs. voltage v across the specimen Pb-46 showing phonon structure at 0.34°K.

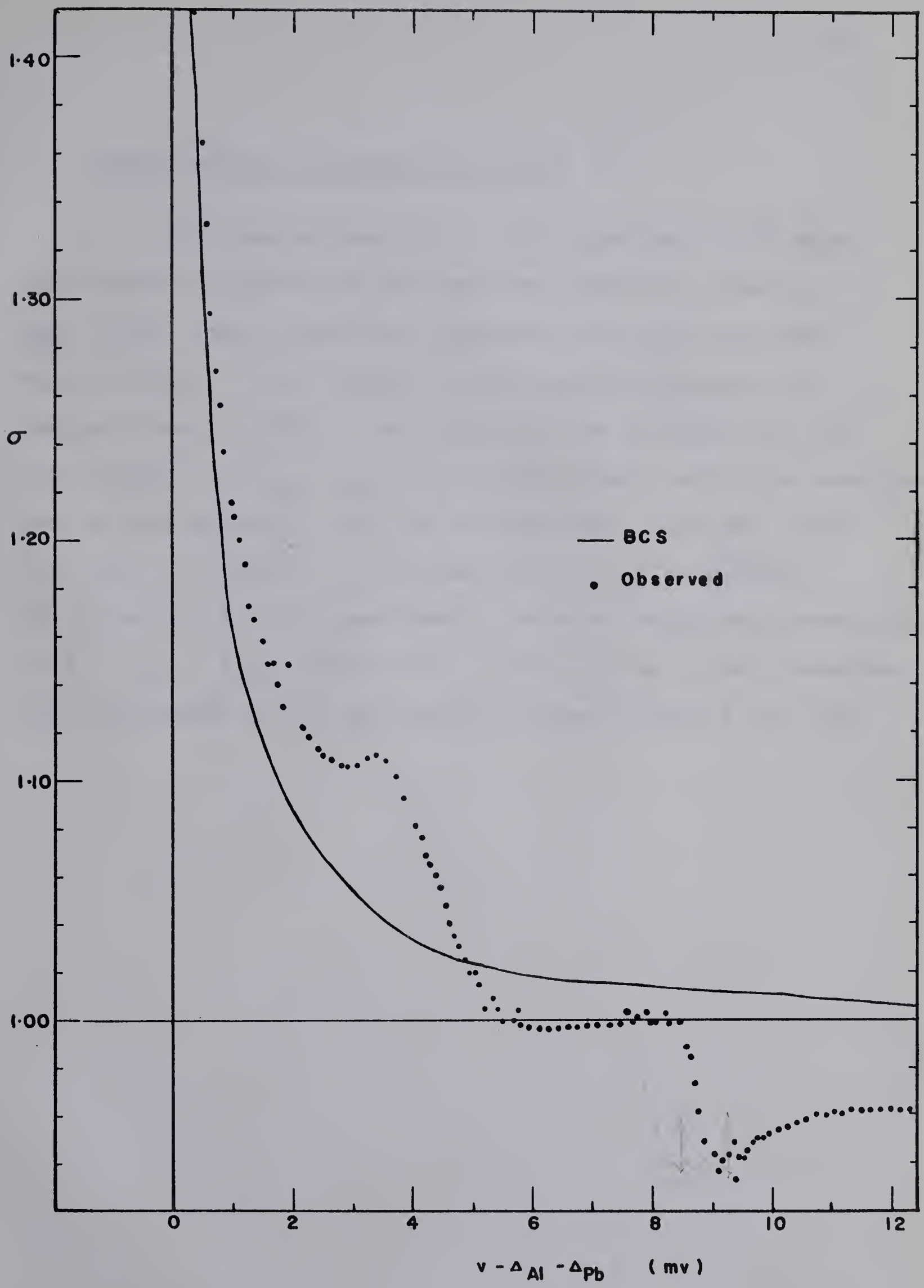
1·40
1·30
1·20
1·10
1·00
σ
BCS
Observed
0
2
4
6
8
10
12
v - Δ Al - Δ Pb (mv)

C. Phonon Density of States for Lead

The observations for σ:v for specimen Pb-46 were also taken at 0.34°K and the results, which are shown in Fig. (5.8), are in excellent agreement with the published work of Rowell et al (1963) and the results reported in Rogers' thesis (1964). The origin on the voltage axis has been chosen at $(\Delta_{Al} + \Delta_{Pb})$ so that the phonon structure energies can be read directly from the voltage axis. The BCS curve for $\Delta(E)$ = constant = Δ_o is also plotted for comparison. The structure in the experimental curve at energies corresponding to $(v - \Delta_{Al} - \Delta_{Pb})$ equal to 4.5 mv and 8.5 mv is well resolved and corresponds to the predominant phonon energies for lead.

CHAPTER VI

CONCLUSIONS

A. Results for Lead

A peak in the effective tunneling density of states in Pb due to recombination effects has been found. It is reflected as an additional peak near 3.9 mv in the normalized dynamic conductance curve for a tunnel junction containing lead. Our results are in agreement with the calculated results of Scalapino et al (1965). The variation of the recombination effect with temperature has also been studied. The recombination effect has been found to be most prominent just below T_c. The slight difference between our experimental values and the calculated values of Scalapino et al (1965) for σ at the gap edge could not be decisively explained.

B. Thermometry Results

An interpolation formula with three unknowns has been found suitable for a germanium thermometer for temperature calibration in the range of temperatures from nearly 7.2°K to 0.52°K. Temperatures calculated with this equation are accurate to ±0.05°K above 2.5°K and to nearly 1% below 2.5°K.

C. Suggestions for Further Work

During the course of the present work the following experiments, which could provide more definite information, were thought to hold promise for future work:

(i) A study of the variation of the transition temperature with the thickness of Pb film. This should reveal information on the mechanism involved in the change of transition temperatures of the films from that of the bulk value. We have found that the transition temperature of Pb, a strongly coupled superconductor, in thin films is lower than its transition temperature in bulk. In comparison, the transition temperature of Al, a weakly coupled superconductor, is higher in thin films than its transition temperature in bulk. Thus the difference in the transition temperature of the film and of the bulk material may depend on the strength of the electron-phonon interaction.

(ii) A search for recombination effects and a study of the phonon density of states in Hg. This ~~It~~ is interesting because it is a strongly coupled superconductor like Pb. It has been only slightly investigated due probably to difficulties in preparation of a Hg specimen.

(iii) Use of Mg as a base layer metal. Mg will remain as a normal metal at all lower temperatures. The electron density of states in a normal metal does not appear in the σ:v curve (cf. Chapter III) and hence a N-S system with a base layer of Mg will be helpful in the study of the phonon density of states of the superconducting member of the tunnel junction.

REFERENCES

Adkins, C. J., 1963. Phil. Mag. 8, 1051.

Adler, J. G., 1963. Electron Tunneling Into Superconductors. Doctoral Thesis, University of Alberta.

Bardeen, J., 1961. Phys. Rev. Letters 6, 57.

Bardeen, J., Cooper, L. N. and Schrieffer, J. R., 1957 a. Phys. Rev. 106, 162.

Bardeen, J., Cooper, L. N. and Schrieffer, J. R., 1957 b. Phys. Rev. 108, 1175.

Bogoliubov, N. N., Tolmachev, V. V. and Shirkov, D. V., 1958. A New Method in the Theory of Superconductivity (translation: Consultants Bureau, New York, 1959).

Clement, J. R. and Quinnell, E. H., 1952. Rev. Sci. Instrum. 23, 213.

Cochran, J. F. and Mapother, D. E., 1958. Phys. Rev. 111, 132.

Cohen, M. H., Falicov, L. M. and Phillips, J. C., 1962. Phys. Rev. Letters 8, 316.

Cooper, L. N., 1956. Phys. Rev. 104, 1189.

Dauphinee, T. M., 1953. Can. Jour. Phys. 31, 577.

Eliashberg, G. M., 1960. Soviet Phys. JETP 11, 696.

Fisher, J. C. and Giaever, I., 1961. Jour. Appl. Phys. 32, 172.

Franck, J. P. and Martin, D. L., 1961. Can. Jour. Phys. 39, 1320.

Giaever, I., 1960 a. Phys. Rev. Letters 5, 147.

Giaever, I., 1960 b. Phys. Rev. Letters 5, 464.

Giaever, I., Hart, H. R. Jr. and Megerle, K., 1962. Phys. Rev. 126, 941.

Giaever, I. and Megerle, K., 1961. Phys. Rev. 122, 1101.

Harrison, W. A., 1961. Phys. Rev. 123, 85.

Onnes, H. K., 1911. Leiden Comm. 122 b, 124 c.

Nicol, J., Shapiro, S. and Smith, P. H., 1960. Phys. Rev. Letters 5, 461.

Martin, D. L., 1961. Proc. Phys. Soc. 78, 1482.

Rogers, J. S., 1962. The Lorentz Number of Aluminum. M.Sc. Thesis, University of Alberta.

Rogers, J. S., 1964. Electron Tunneling into Superconductors. Doctoral Thesis, University of Alberta.

Rogers, J. S., Adler, J. G. and Woods, S. B., 1964. Rev. Sci. Instrum. 35, 208.

Rowell, J. M., Anderson, P. W. and Thomas, D. E., 1963. Phys. Rev. Letters 10, 334.

Scalapino, D. J. and Anderson, P. W., 1964. Phys. Rev. 133, A921.

Scalapino, D. J., Wada, Y. and Swihart, J. C., 1965 a. Phys. Rev. Letters 14, 102.

Swihart, J. C., Scalapino, D. J. and Wada, Y., 1965 b. Phys. Rev. Letters 14, 106.

Schrieffer, J. R., 1964. Theory of Superconductivity (Benjamin, Inc., Publishers, New York).

Schrieffer, J. R., Scalapino, D. J. and Wilkins, J. W., 1963. Phys. Rev. Letters 10, 336.

Schrieffer, J. R. and Wilkins, J. W., 1963. Phys. Rev. Letters 10, 17.

Shapiro, S., Smith, P. H., Nicol, J., Miles, J. L. and Strong, P. F., 1962. I.B.M. Jour. Research and Development 6, 34.

Taylor, B. N. and Burstein, E., 1963. Phys. Rev. Letters 10, 14.

White, G. K., 1959. Experimental Techniques in Low-Temperature Physics (Oxford University Press).